PHYTOCHEMICALS AND REPURPOSED, FDA APPROVED DRUGS SHOW POTENTIAL AS A COST EFFECTIVE COMBINATION TREATMENT FOR OVARIAN CANCER

By CHASE TYLER CHRISTENSEN

A thesis submitted to

the School of Graduate Studies

Rutgers, The State University of New Jersey

In partial fulfillment of the requirements

For the degree of

Master of Science

Graduate Program in Cell and Developmental Biology

Written under the direction of

Dunne Fong

And approved by

_____

_____

_____

New Brunswick, New Jersey

May, 2020

ABSTRACT OF THE THESIS

PHYTOCHEMICALS AND REPURPOSED, FDA APPROVED DRUGS

SHOW POTENTIAL AS A COST EFFECTIVE

COMBINATION TREATMENT FOR OVARIAN CANCER

by CHASE TYLER CHRISTENSEN

Thesis Director:

Dunne Fong

A cancer diagnosis is an event that countless people fear. Besides the debilitating effects of the disease itself, treatments also take a substantial toll on a patient's health as well as their finances. Even successful treatments cause survivors to live with the constant concern that their illness will return. When relapse does occur, prior therapies may no longer be an option due to cancer cells gaining resistance under the cancer stem cell model. As such, new therapies must be developed to once again aid patients enter a second battle for their lives.

Phytochemicals, for example curcumin, are plant derived molecules that have shown promise as a potential treatment for ovarian and other cancers. In addition to phytochemicals, repurposed FDA approved drugs are another option being explored by researchers. Studying drugs that are already approved for other indications will reduce the time and cost required to develop new therapies. For people living with limited access to medical care due to financial matters, low cost treatment for deadly diseases is highly desired.

By conducting a series of *in vitro* alamarBlue cell viability assays, this paper aims to provide evidence that niclosamide, an off patent FDA approved drug for parasitic tapeworm infection, and curcumin, a phytochemical derived from turmeric, hold the potential to be low cost therapies for women suffering from ovarian cancer. In addition, using these molecules in combination has shown synergistic properties that act to decrease cell viability of SKOV3 ovarian cancer cells. Under the cancer stem cell model, cases of relapse may be reduced by using niclosamide and curcumin to target resistant subpopulations of cancer cells left after conventional therapies are administered.

Acknowledgements

I would like to thank Dr. Dunne Fong for the countless times he has helped me throughout my career at Rutgers University. During the last 4 years, I have learnt more than I could have ever imagined. It was your Advanced Cell Biology Laboratory course that introduced me to scientific research. In spite of the fact I was an undergraduate student in my final semester and void of any prior research experience, you gave me a chance whereas other professors declined or flat out ignored my requests since sophomore year. It was with your help that I entered into graduate school and received my teaching assistant position for the same course that started me on this path. The techniques I learnt in your laboratory changed me from being a person in possession of a science degree into a person who can finally call himself a scientist. Once again, thank you for everything you have done over the years.

I would also like to thank Dr. Kelvin Kwan and Dr. Arash Hatefi for providing our lab with their expertise and materials that contributed to our research. Dr. Dongming Sun has helped our lab on numerous occasions, be it course work or my research. I truly appreciate the time he has spent assisting us in imaging cells. There are countless others who I have had the pleasure of meeting during my time at Rutgers. Our interactions left lasting marks that will be carried with me wherever I may find myself in the future.

Funding for Dr. Dunne Fong's lab and the experiments conducted for this thesis were obtained through a grant from the New Jersey Health Foundation.

Table of Contents

List of Tables

List of Illustrations

Introduction

The diagnosis of cancer is perhaps the most feared outcome that a patient can receive when seeking medical care. The general perception of the disease stems from its persistent and aggressive nature as well as the debilitating effects that both the disease and treatment methods have on the human body. Sadly, many people usually lack a strong understanding of the causes, complexity, and treatment possibilities until they or a loved one has received this earth shattering news. However, many people are painfully aware of the high medical cost associated with cancer care.

In order to understand the disease, one must first understand that cancer is a very broad term that needs classification to give meaning to a diagnosis. As such, many people are aware that medical professionals classify cancers by tissue type and stage of disease progression. While the general concept of abnormally high cellular proliferation lacking regulation is the basis for defining cancer, there are numerous underlying causes for this to occur. For example, ovarian cancer cells may exhibit one or more genetic mutations that influence their ability to properly check for DNA damage during mitosis. Even events like chromosomal translocations, such as the atypical exchange of regions between chromosomes 22 and 9 linked to acute lymphoblastic leukemia, show a different mechanism that results in a cancerous state.

Furthermore, understanding how specialized cells differentiate from stem cells during embryogenesis also brings about insight as to the level of complexity the exists in the broad disease referred to as cancer. Another set of dynamic issues occur when genes are selected for silencing or activation to produce a specific cell type. Having hepatocytes, glial cells, and muscle cells display different gene expression patterns is an evolutionary necessity for each cell type to fit its function. But this is problematic when it comes to treating cancer cases. The heterogeneity of gene expression that

exists among cell types makes finding a single, widely applicable therapeutic target a challenge for drug developers. The fact that cancer cells within a single tumor may express different mutations from one another only exacerbates the situation (Mackillop, 1983). The cancer stem cell (CSC) model explains the various populations of cells that exist in a tumor. Under the model, cancer stem cells are a subpopulation of tumor cells which express stem-like characteristic, e.g. self-renewal, responsible for tumorigenesis and development of drug resistance (Fong, 2010)(Du, 2009). Finding compounds that target CSC populations should reduce the likelihood for patients to experience a relapse. Consideration of all the mentioned concepts is necessary to form a more detailed understanding of cancer which in turn focuses on characteristics that may serve as precise targets for future therapeutics.

Background

With an understanding of the complexities associated with cancer, it is best to avoid thinking of it as one disease. Instead, viewing it as a compilation of diseases better reflects the diversity previously discussed. This train of thought provides better clarity when contemplating characteristics of cancers, such as processes by which cells develop drug resistance making future treatment more difficult. From here scientists have two clear options in countering these drug resistant cells. The first line of action is to find out the mechanism these cells used to obtain resistance and to target the mechanism with a secondary drug or biologic. However, this may not be the most effective, efficient, nor marketable way to approach a given cancer type. It is possible that a mechanism of resistance may only be attributed to a minuscule subpopulation of ovarian cancer cases. If it is true that the mechanism is not commonly expressed in other cancerous tissue types then the treatment may be overlooked by developers in favor of a more inclusive, yet inferior, drug target. This is why most researchers and companies follow the second route of attempting to find a new drug that targets cancer cells at a common key cellular process. If the new drug works in a novel way or on a novel target involved in DNA synthesis, ATP synthesis and utilization, or by increasing cancer cell sensitivity to other drugs then a wider-range of cancer types can be treated. Thus, this new wide-range drug would be a more desired project for pharmaceutical companies to pursue. Cisplatin and Taxol (paclitaxel) are examples of drugs effective against multiple cancers. Both of these drugs are used in the treatment of ovarian, breast and lung cancers (Ovarian Cancer Treatment, n.d.).

Being aware of cancer's complex nature also highlights the importance in developing new therapeutic treatment options. Using drugs in combination allows for

a more effective therapy indented to prevent future relapses by expanding the number of cancer cells targeted during a patient's initial treatment. The use of phytochemicals, biologically active compounds derived from plants, might be a promising strategy to deploy alongside conventional cancer therapies.

If focus is paid to ovarian cancer then it is clearly shown how complexity influences therapeutic regimens. To begin, the 1 in 75 occurrence rate for ovarian cancer places it 8th in terms of commonality and 5th in cancer fatalities for women (Statistics, n.d.). It is also unfortunate that many cases are not caught until they have progressed into later stages. The failure in identifying ovarian cancer is due in part to the difficulty in detecting the cancer in patients until symptoms increase in severity. The issue of a low early detection rate also lies with the anatomy of the ovaries and adjacent structures. The ovaries' small size (approximately 3 cm) and their location within the abdominal cavity make detection of abnormalities difficult. Symptoms associated with the disease are nondescript and are also easily mistaken as non-life-threatening ailments. Ovarian cancer is commonly derived from the three cell types: epithelial cells lining the ovaries, germ cells for reproduction, and stromal cells that provide structural support to the ovaries and produce female hormones (Thomas, 1998)(Du, 2009). A study has found 5-15% of ovarian cancer patients possess mutation in BRCA1 and BRCA2 tumor suppressor genes (Ramus, 2009). Defects in these genes cause a diminished ability for cells to repair DNA damage and can result in the accumulation of additional mutations leading to cancer (BRCA Mutation, n.d.).

Conventional cancer treatments, i.e. radiation, chemotherapy, and surgery, remain crucial lifesaving options. As previously mentioned, cisplatin and paclitaxel are two chemotherapeutics used to disrupt a cancer cell's proliferative abilities. Cisplatin works by interfering with the cell's DNA repair mechanism through the formation of

a crosslink between the drug and purine bases leading to DNA damage that will signal the cell to undergo apoptosis (Dasari, 2014). Paclitaxel's molecular targets are the microtubules responsible for binding and separating sister chromatids during mitosis. Microtubules consist of many α and β tubulin heterodimer units. These heterodimers are added at the polymerization end of the microtubule and are released at the depolymerization end. This energetic pairing of elongation and curtailment will create the pulling motion that is responsible for chromosomal segregation after microtubules have anchored to the kinetochore and centrosome. However, paclitaxel inhibits disassembly of heterodimers from the microtubule's depolarization end causing interference with kinetochore attachment and activation of the mitotic checkpoint (Weaver, 2014). The mitotic checkpoint will detect if there is an asymmetric attachment of microtubules to kinetochores eventually leading to cell cycle arrest (Waters, 1998). It is important to note that these drugs are not cancer cell specific. In other words, damage to healthy tissue is a side effect of drug treatment. Hair loss, vomiting, and gastrointestinal (GI) bleeding comprise some of the common ailments. These symptoms are caused by the off target inhibition of a normal, healthy cell's reproductive ability within regions that have high turnover rates needed to maintain follicle growth or act as a protective coating to the GI tract.

Radiation is used to destroy cancer cells by damaging DNA either through internal or external procedures. One method, brachytherapy, utilizes a radioactive source in the form of an implantable device placed within afflicted tissue (Radiation Therapy, n.d.). Emitted radiation targets cancer cells in the surrounding area. On the other hand, external treatment is given through the use of a photon beam generated by a machine and coupled to a series of preliminary calculations and measurements

ensuring accurate and precise delivery of gamma or x-rays to a location within the patient's body (Radiation Therapy, n.d.).

The last of the conventional therapies used to treat ovarian cancer is surgery. While the idea of physically removing the cancerous tissue may seem like the most logical and straightforward approach, it is actually much more complex than it appears. Specialized surgeons called gynecologic oncologists are responsible for carrying out the procedure and suggesting follow up treatments based on their observations. The goals set during surgery include debulking, or in other words removing the cancerous mass with priority assigned to tumors over 1cm in size, and staging, determining if the cancer has spread to adjacent tissues or metastasized to distal regions of the body (Ovarian Cancer Treatment, n.d.). Early staging may involve transvaginal ultrasounds to allow for a pre-surgical strategy on debulking. Modification to the extent of debulking will depend on staging made by the surgeon during the operation. It may be deemed necessary to remove the ovaries and the fallopian tubes, i.e. a bilateral salpingo-oophorectomy, or the uterus may also need to be extracted via a hysterectomy. Other circumstances, like if a patient wishes to retain an ovary so that she could have children, will also impact the plan for debulking. A more detailed staging report will be performed through biopsies of tissue collected during surgery. Due to the possibility of lab result discovering a patient's cancer has spread to other tissue, it may be imperative to follow up with another surgical procedure or a different treatment option, i.e. chemotherapy.

Alongside the conventional therapies are biologic options including hormone and targeted therapies. An example of a targeted therapy is bevacizumab, also known by its brand name Avastin. This treatment employs monoclonal antibodies against vascular endothelial growth factor (VEGF) to prevent said growth factor from binding

cell surface receptors (Genentech, n.d.). The ability to inhibit VEGF classifies Avastin as an anti-angiogenic agent designed to starve tumors of a sufficient blood supply in order to prevent cancer progression. Avastin's mechanism of action is based on the findings that tumors develop hypoxic conditions in their cores once they have reached 1-2 mm^2 in size (Hillen, 2007). At this stage in tumorigenesis VEGF is released by tumor cells to promote angiogenesis in the area surrounding the tumor as a strategy to counteract hypoxia by increasing oxygen supply. Avastin is a preferred treatment for late stage or metastatic cancers since the increased production of VEGF is a hallmark of large tumors or those with cells undergoing epithelial-mesenchymal transition (EMT). During EMT cells become depolarized as a means to break free from the tumor and enter the enhanced vascular system surrounding it. By doing so, cancer cells can spread within the circulatory or lymphatic systems until they reach a distant tissue in which secondary tumorigenesis may occur.

The use of combination therapy is commonly seen in ovarian cancer treatment. The idea revolves around attacking the cancer on two fronts. If a patient receives a combination of two therapies with different molecular targets then there is an increased likelihood of successful outcome. A study was conducted to test the combination of three therapies: a demethylating agent called decitabine, the chemotherapy drug doxorubicin, and a cancer vaccine containing NY-ESO-1 protein with Montanide and GM-CSF (Odunsi, 2014). By using multiple treatment options, it is possible to make cancer cells more susceptible to a conventional therapy. It is also possible that a combined therapy may even target subpopulations of cancer cells that express different genetic mutations. The procedure was tested on a group of patients who had recurrent ovarian cancer with a developed chemotherapeutic resistance. The results showed that 60% of the patients in the phase 1 clinical trial had responded to

the treatment with 5 patients' cancer becoming stable for 7.8 months and 1 patient being in a state of remission for 5.8 months (Odunsi, 2014). The combination of therapies was also heavily depended on timed dosages and the order in which the therapies were administered. For example, if decitabine was given after chemotherapy then the procedure was shown to be ineffective.

Inspirations for Research

An interesting topic in the combination approach for treating cancer is the prospect of using phytochemicals. Phytochemicals are biologically active compounds originating in plants and whose dietary intake aid in protection against diseases (Yoo, 2018). Compounds isolated from plants, e.g. Taxol (paclitaxel), already exists as pharmaceuticals and there remain many others that have shown promise when tested *in vitro*. Even though supporting data collected from workbench studies exist, there is a lack of extensive clinical trials being performed to gather evidence of *in vivo* efficacy of phytochemicals on cancer. Some of the compounds that have shown promise in the laboratory include curcumin, a yellow polyphenol from turmeric, epigallocatechin gallate (EGCG) found in green tea, and resveratrol isolated from fruits like grapes and berries (Fong, 2013).

Curcumin, as well as other phytochemicals, have received Generally Recognized as Safe (GRAS) designations from the Food and Drug Administration (FDA) (GRAS Notices, 2019). Investigations into dietary intake of curcumin have shown it to be an effective chemopreventive and antioxidant (Mohandas, 1999). Researchers have expanded on this observation by designing experiments to test curcumin on cancer cells with hopes of identifying a potential new treatment. Results have shown two of

curcumin's modes of action are to inhibit the NF-κB and STAT3 signaling pathways associated with cancer progression (Vallianou, 2015). Based on the finding of STAT3 inhibition, it is suggested that curcumin inhibits ovarian cancer growth and stimulates apoptosis (Yallapu, 2010).

Research data from *in vitro* experiments have generated compelling evidence of the potential for new cancer treatments involving phytochemicals. Yallapu (2010) focused on an ovarian cancer cell line, A2780cp, that had developed cisplatin resistance. Figure 1A depicts the experimental design using A2780cp monolayer cultures treated with curcumin and cisplatin. Figure 1B indicates cultures were grown with either 10 μM or 20 μM of curcumin along with variable concentrations of cisplatin. Controls for cisplatin and curcumin were also included.

The results of the study indicate that curcumin either increased the sensitivity of the cells to cisplatin or had its own mode of action responsible for a decrease in proliferation. The combination of the two drugs in figure 1C suggest a more powerful outcome on the percentage of proliferation of A2780cp cells than either drug possessed when tested independently.

Figure 1

Yallapu's Combination Study for Curcumin and Cisplatin

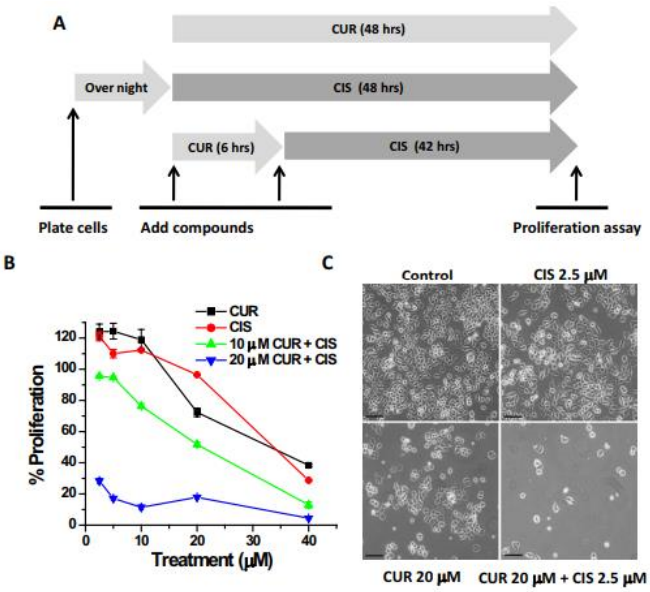

Note. A2780cp results for monolayer cultures treated with curcumin (CUR), cisplatin (CIS), or a combination of drugs. A) Explanation of experimental design for timing of drug delivery and assay. B) Effects on cell proliferation due to dosing. C) Images of wells depicting differences in cell culture proliferation. Figure 1 was found on page 5 of the *Journal of Ovarian Research* publication of *Curcumin Induces Chemo/Radio-Sensitization in Ovarian Cancer Cells and Curcumin Nanoparticles Inhibit Ovarian Cancer Cell Growth* by Yallapu, 2010.

There also exists off patent, FDA approved medications intended to treat various disease, but have also shown signs of being anti-cancer agents. One such medication, niclosamide, is used in treating parasitic worm infections, making it a member of the anthelmintic group of drugs (Niclosamide, 2020). Niclosamide is a drug capable of inhibiting mTORC1 and Notch signal pathways as well as the NF-κB and STAT3 pathways characteristic of curcumin's function (Li, 2014). *In vitro* and *in vivo* studies

testing a range of doses from 0.75 μM to 6 μM were shown to have effects on ovarian cancer cell viability (Yo, 2012).

Scope of Thesis

Even though numerous treatment methods and pharmaceutical products exist to combat cancer, the overall fight is still severely lacking the tools necessary to take control of the war. New discoveries and drug approvals continue to add more options for physicians and their patients. The number of high risk invasive procedure may decrease as more effective therapeutic methods reach the market. Conventional chemotherapy may serve as the groundwork for a strategy that combines top tier therapies with other drugs to enhance the sensitivity of persistent cancer stem cells. Creating a plan that attacks cancer on multiple fronts may lead to a more efficient first line of treatment for patients and reduce the chance of relapse caused by cells able to evade their eradication.

The cost of cancer treatment is a serious concern for many patients. A study of 5,031 insured ovarian cancer patients found the median cost of surgical procedures to be $30,708 with trailing 12-month expenses bring the total cost to $93,632 (Bercow, 2017). Costs of treatment significantly increased when conventional therapies were used in combination. In 2009 a study involving 100 patients who received debulking procedures followed by chemotherapy found the average medical cost was $211,940 (Christophe, 2009). Even with health insurance many people may still be responsible for tens of thousands of dollars in medical bills. On the global scale, the vast majority of people do not have any means to meet these costs. The best hope for many of these people is the creation of low cost treatments which come in the form of non-patentable, naturally occurring compounds or FDA approved medications that no longer have exclusivity. Niclosamide and curcumin are both low cost compounds with a price of $1.12 per gram and $3.10 per gram, respectively (Curcumin, n.d.)(Niclosamide, n.d.).

Research into curcumin and niclosamide combination therapy has multiple benefits to society. If a therapy were to be developed using these two low-cost compounds then cancer treatment may become available to millions more people who otherwise would not be able to afford it. Again, every new therapy adds an additional option to the physicians' pharmaceutical war chest when devising a patient's treatment strategy. Perhaps curcumin-niclosamide dosing is used in combination with first line therapies to target CSC in order to reduce the likelihood of relapse. If not, it may still be used down the line in treatment of cases were cancers are resistant to the gold standard drugs. Studies must first begin *in vitro* before any of these suggested future uses can be possible. As such, new experiments focused on the effects of these compounds on ovarian cancer have been performed and are discussed within this paper. Provided alongside results are extensive details allowing others to reproduce experiments from this study with an exact understanding of how the procedures were performed.

Methods and Materials

Passaging of Tissue Culture Flasks

Ovarian cancer cell line SKOV3 was used in the curcumin-niclosamide combination study. The cell line was cultured in a growth medium consisting of 89% Roswell Park Memorial Institute (RPMI) 1640, 10% fetal bovine serum (FBS), and 1% penicillin-streptomycin (Pen-Strep). Cultures were grown in either T-25 or T-75 treated flasks under incubation settings of 37°C and 5% CO_2. The procedure for cell line maintenance was conducted as follows:

1. Under sterile conditions, a T-25 flask (ideally being in the range of 70%-80% confluence) was decanted into a 10% bleach solution in order to remove the growth medium.
2. 5 mL of a saline wash (0.9% NaCl) was then added to the flask, gently swirled, and decanted to remove residual growth medium.
3. 0.5 mL of Trypsin-EDTA (0.25%) was added to the flask before incubating for 1 minute at 37° C.
4. After incubation, the flask was inspected using a microscope to ensure successful trypsinization. This was indicated by the contraction/rounding of cells that form the monolayer. As a result, a noticeable gap between cells could be observed. The flask was then tapped by hand and occasionally swirled to assist in detachment of cells.
5. The flask was then held at a steep angle as 5 mL of growth medium was passed over the surface where monolayered cells were previously attached. The now neutralized trypsin-cells-medium mixture pooled at the bottom of the flask was immediately transferred to a 15 mL centrifuge tube.

6. The 15 mL centrifuge tube containing the suspended cells were centrifuged at room temperature for 5 minutes at 1000 RPM.
7. After centrifugation, the supernatant was decanted from the 15 mL centrifuge tube. The pelleted cells were then resuspended in 1 mL of growth medium.
8. Finally, a new T-25 treated flask was filled with RPMI and an appropriate portion of the resuspended cells (see section titled *ensuring subconfluence of tissue culture flasks*) so that the final volume reached 10 mL. The flask was then oscillated by hand to disperse the seeded cells before it was placed into the incubator.

Ensuring Subconfluence of Tissue Culture Flasks

Since the assay used in the drug combination study relies upon measuring the metabolic activity of cells to determine treatment effectiveness, it was vital to ensured cells used in these experiments were in a similar state each and every time a well plate was ran. If the monolayer cultures were allowed to become overgrown (>80% confluent), then contact inhibition of proliferation may influence results from week to week by interfering with the rate of proliferation (Mendonsa, 2018). Maintaining flasks under 80% confluence acted to prevent this variable from impacting data. A series of steps were designed to control the rate at which flasks reached confluence. This system worked very well to form a reliable laboratory schedule used to maintain cell lines in T-25 or T-75 flasks.

The flask was inspected by eye and through the use of a compound light microscope before passaging. Vigilance was paid towards signs of excessive debris, dead cells, or possible signs of contamination that indicate the culture was unhealthy

and unfit for use. Properly maintained, subconfluent flasks should have little to no debris present. Growth medium, in this case RPMI, containing phenol red was visually inspected for favorable pH conditions when maintaining the cell cultures.

It was crucial that multiple regions of the monolayer were inspected when determining confluence. Improper techniques when seeding cells or differences in flask manufacturing may contribute to uneven growth of the monolayer. Even with proper seeding techniques, some regions of the flask may appear more confluent than others. Typically, this can be witnessed along the edges of the flask. If ignored, these high density regions could become overgrown while the center region of the flask may wrongly indicate subconfluence. When determining the degree of confluence, consideration should be made for regions of varying cell density in an effort to estimate an average percent confluence.

Passaging of the flasks followed the procedure previously outlined. When the trypsinization step was reached, dissociation of cells from the monolayer could be done by tapping the flask from both sides with gently swirling motions interspersed. A microscope was utilized to check cell detachment from the flask. Attention was paid to the flask's edges as cells growing here require more effort to be freed from the monolayer. Tilting the flask and allowing the trypsin to collect at the edge while tapping the side allows for easier detachment of lingering cells.

By adding medium directly to the flask and transferring the entire volume of the trypsin-cell-medium mixture to a centrifuge tube, a researcher can increase the efficiency of cell collection. The addition of growth medium acts to decrease the cell density through increasing volume. Thus, a larger number of cells can be collected by reducing the density of residual fluid found remaining in the flask. More importantly,

adding growth medium allows for alpha-2-macroglobulin, a component of FBS, to bind and neutralize the effects of trypsin. Centrifugation of the mixture was used to remove the neutralized trypsin before cells were resuspended in fresh growth medium.

It is common to see researchers create subcultures by simply taking a portion of the harvested cells, say 1/4th the pelleted cells, and adding it to a new flask. This method is not truly reliable when it comes to cell line maintenance as it does not account for the confluence of the flask the cells were harvested from. For example, a new flask which received 1/4th of the cells from an 80% confluent flask will reach a point of overgrowth faster than if 1/4th of the cells from a 40% confluent flask were used. In order to establish a reliable work schedule for laboratory experiments, a short calculation could be made before subculturing. The principle for this calculation originates from the idea that a flask should not exceed 80% confluence. With this number in mind, a short equation was created.

$$\frac{80}{X} \times Y \quad = Z$$

Here we see that the numerator is set to equal the maximum allowed confluence. The denominator X is defined as the observed confluence of the flask being passaged. The value Y represents a volume for the portion of resuspended cells the researcher desires to use in subculturing. The sum Z is the adjusted volume where confluence of the passaged flask is considered. This equation acts to normalizing the number of cells added to a flask to ensure confluence does not exceed 80% at the time said flask is intended to be used.

This equation is designed to help researchers ensure a flask does not exceed its maximum allowed confluences all the while allowing for a predictable maturity date based on research schedule. Because cell lines differ in characteristics, such as

morphology and rate of growth, the Y value will have to be determined through a researcher's experience with the cell line and their desired date for the flask to reach maturity. Modifications can be made to the numerator in the event a different desired confluence is selected.

A quick example highlights how the equation is intended to be used. Suppose a researcher was in possession of a 60% confluent flask. The researcher would like an 80% confluent subculture to be ready in 72 hours. Based on experiences passaging 80% confluent flasks, the collected pellet would be resuspended in 1 mL of medium and seeding of 250 μL allowed for a subculture to be ready on time. If the researcher decided to use the 60% confluent flask then X=60, Y=250 μL, and the Z value would be approximately 333.3 μL meaning more volume would have to be added when preparing the subculture. This acts to compensate for the fewer number of cells present due to a lower level of confluence than typically preferred.

Cell Counting

Cells were counted using a hemocytometer in combination with trypan blue. Passaging of a flask yielded a centrifuge tube containing pelleted cells ready for resuspending in growth medium (see section titled *passaging of tissue culture flasks,* step 7). Attention was paid to confirm pellet had been completely dissolved in medium through cyclical pipetting. One blank well of a 96-well plate was used to mix an equal part of trypan blue to that of resuspended cells. Typically, this was a 50 μL to 50 μL mixture. During mixing, the pipette was held in a manner to prevent the tip from resting against the sides or bottom of the well. Taking this measure prevented

obstruction of the tip as the solutions were gently mixed by pipetting approximately 6 times up and down.

The hemocytometer was primed by delivering 10 μL of the cell-trypan blue mixture to each counting chamber. The entire 1 mm^2 grid etched into the hemocytometer was used for count. During the counting process, cells that were observed to be laying on or touch the lines marking the 1 mm^2 perimeter had to be approached in a logical manner. If all cells laying on or touching the 4 sides of the grid were counted, then the number recorded would be inaccurate due to artificially expanding the boarders of the grid beyond that on the 1 mm^2. It was decided that only cells laying on or touching 2 out of the 4 sides would be included in the final count. In theory, this acted to shifted the grid in a way that only 1 mm^2 of area was counted. An alternative option that could have been used was to only include 1/2 of the cells laying on or touching the perimeter when forming a final count.

Each of the two counting chambers were double counted. This measure ensured no mistakes were made when observing independent chambers, and that there were no major discrepancies between the two chambers. An average was taken from the numbers that were generated. A dilution factor of 2 had to be considered due to mixing equal parts trypan blue and cells suspended in medium. Another number critical in this process was $1.0x10^4$ which acts to convert the number of cells counted to a density given for 1 mL of the resuspended cells. This number derives from the fact that the volume above the 1 mm^2 grid that was contained between the hemocytometer and coverslip equated to .1 μL. Utilizing these 3 values made it possible to calculate the number of cells in a given volume, i.e. of the 1 mL of resuspended cells obtained from passaged flask.

96-Well Plate Preparation

Corning Costar (3596) TC-Treated 96-well plates were utilized in this drug-phytochemical combination study. A flask would be passaged, the collected cells counted, and a 96-well plate would be prepared for the *in vitro* study. Wells along the outer edge of the plate were not used in collecting data due to possible interference caused by evaporation. This phenomenon, called the edge effect, may influence experimental results through an increase in solute concentration, in this case drug product and/or phytochemical, caused by a decrease in solvent volume, e.g. growth medium (Neeley, 2016). To eliminate this phenomenon's potential influence on data collected during the study, the outer wells received 100 µL aliquots of medium in an effort to humidify the plate in combination with an open, sterile water tray placed inside the incubator.

The central 60 wells were used to conduct the drug-phytochemical combination study. Experimental design called for the addition of 3,000 cells per well, except for the blank control wells where only growth medium would be present. Preparation of the plate was performed by taking an aliquot of counted cells and adding it to a larger volume of growth medium contained in a centrifuge tube. The necessary volumes to create this mixture were calculated based on 60 wells containing a final volume of 100 µL per well. By combining appropriate amounts of growth medium and counted resuspended cells, a more uniformed sample of cells suspended in medium was created and used to fill the 60 central wells with the intended 3,000 cells per well. The centrifuge tube was periodically capped and inverted during the pipetting process as a means to ensure cells did not precipitate to the bottom. This action was implemented to reduce the likelihood of variation in cell count per well.

The 96-well plate was visually inspected after the pipetting process to make certain errors were not made. Visual inspect was a simple means to ensure correct volumes had been added to both the outer wells containing medium and inner wells containing diluted cell stock. Since distribution of either growth medium or diluted cell stock utilized a pipette fixed at 100 μL, a misplacement of an aliquot would produce an obvious abnormality in the plate where volume would be twice as great as intended.

Following inspection and labeling, the 96-well plate was place into incubation at 37°C and 5% CO_2. The plate was examined by microscope after 24 hours. Wells were inspected for signs confirming monolayer formation and absence of any contaminants. It is at this point the plate would enter the second stage of the experiment by receiving doses of the pharmaceutical products and phytochemicals.

Drug Stock Preparation and Addition to 96-Well Plate

A 5 mM master stock of niclosamide was prepared by dissolving the compound in dimethyl sulfoxide (DMSO). DMSO was also used as the solvent to create a curcumin master stock also 5 mM in concentration. A 0.2 mg/mL cisplatin stock was made using sterile water as its solvent. The three master stocks were divided into smaller portions, based on need, then frozen. Having multiple smaller volumes prevented repetitive freeze-thaw cycles that could cause compounds to degrade (Kozikowski, 2003)(Rayfield, 2017).

A 96-well plate that had been seeded and placed into incubation 24 hours earlier was inspected for early signs of monolayer formation. As always, wells were also checked for any signs of possible contamination before proceeding. Curcumin and

niclosamide 5 mM master stocks would then be used to create working solutions of lower concentration through dilution with growth medium. Niclosamide was diluted to a 20 μM working solution. Curcumin was diluted to an 80 μM working solution. Curcumin and niclosamide working solutions were made fresh before every experiment as storage of bulk drug-medium mixtures at 4°C may result in degradation of the investigational compounds (Naksuriya, 2016).

Information searches that inspired part of this experiment also aided in determining appropriate dose ranges for curcumin and niclosamide. It was decided that curcumin would be tested at 5 μM, 10 μM, 15 μM and 20 μM where as niclosamide would include 0.5 μM, 1 μM, 2.5 μM and 5 μM concentrations (Yallapu, 2010)(Yo, 2012). Cisplatin controls were included at 2 μg/mL and 3 μg/mL concentrations (Chan, 2002). The experimental design allowed controls for each of the four concentration of curcumin and niclosamide, all 16 possible combinations of the compounds, both concentrations of cisplatin controls, a combination of cisplatin and niclosamide, a combination of cisplatin and curcumin, a blank well for calibration when running the alamarBlue assay, and an untreated well containing cells (see table 1). Each plate was organized to include a set of duplication wells permitting two data points to be collected. Having these duplications integrated into the design helped to monitor the experiment for pipetting errors or other discrepancies that would negatively impact the integrity of data.

Table 1

Experimental Design for 96-Well Plates

		Column Number						
Row		1	2, 3	4 , 5	6, 7	8, 9	10, 11	12
	A	X	X	X	X	X	X	X
	B	X	Medium only	Nic 2.5 µM	Cis 2 µg, Cur 15 µM	Nic 1 µM, Cur 5 µM	Nic 2.5 µM, Cur 15 µM	X
	C	X	Cells (Untreated)	Nic 5 µM	Cis 2 µg, Nic 2.5 µM	Nic 1 µM, Cur 10 µM	Nic 2.5 µM, Cur 20 µM	X
	D	X	Cis 2 µg	Cur 5 µM	Nic 0.5 µM, Cur 5 µM	Nic 1 µM, Cur 15 µM	Nic 5 µM, Cur 5 µM	X
	E	X	Cis 3 µg	Cur 10 µM	Nic 0.5 µM, Cur 10 µM	Nic 1 µM, Cur 20 µM	Nic 5 µM, Cur 10 µM	X
	F	X	Nic 0.5 µM	Cur 15 µM	Nic 0.5 µM, Cur 15 µM	Nic 2.5 µM, Cur 5 µM	Nic 5 µM, Cur 15 µM	X
	G	X	Nic 1 µM	Cur 20 µM	Nic 0.5 µM, Cur 20 µM	Nic 2.5 µM, Cur 10 µM	Nic 5 µM, Cur 20 µM	X
	H	X	X	X	X	X	X	X

Note. A representation of the alamarBlue-based cell viability assay detailing the drug and phytochemical concentrations for control and experimental wells. Curcumin (Cur), niclosamide (Nic), and cisplatin (Cis) were used in varying concentrations and combinations. Curcumin doses ranged from 5 µM to 20 µM, niclosamide from 0.5 µM to 5 µM, and cisplatin was used in two concentrations, 2 µg/mL and 3 µg/mL. Duplicate wells were placed in neighboring columns. The outer 36-wells were not used in data collection.

A this point the 96-well plate was ready to receive the appropriate compound dosing according to tables 2, 3, and 4. Each of the 96 wells already contains 100 µL of either medium or cells growing in medium upon entering this stage of the procedure. The 60 central wells received aliquots of curcumin, niclosamide, cisplatin or a combination the stocks.

Table 2

Niclosamide Dosing of 96-Well Plates

	Column Number							
Row		1	2, 3	4 , 5	6, 7	8, 9	10, 11	12
	A	X	X	X	X	X	X	X
	B	X	-	25 µL	-	10 µL	25 µL	X
	C	X	-	50 µL	25 µL	10 µL	25 µL	X
	D	X	-	-	5 µL	10 µL	50 µL	X
	E	X	-	-	5 µL	10 µL	50 µL	X
	F	X	5 µL	-	5 µL	25 µL	50 µL	X
	G	X	10 µL	-	5 µL	25 µL	50 µL	X
	H	X	X	X	X	X	X	X

Note. Numerical values represent volume of 20 µM niclosamide working solution added to designated wells in accordance to table 1. A final volume of 200 µL per well will be reached once all required distributions of drug stocks and medium have been made.

Table 3

Curcumin Dosing of 96-Well Plates

	Column Number							
Row		1	2, 3	4 , 5	6, 7	8, 9	10, 11	12
	A	X	X	X	X	X	X	X
	B	X	-	-	37.5 µL	12.5 µL	37.5 µL	X
	C	X	-	-	-	25 µL	50 µL	X
	D	X	-	12.5 µL	12.5 µL	37.5 µL	12.5 µL	X
	E	X	-	25 µL	25 µL	50 µL	25 µL	X
	F	X	-	37.5 µL	37.5 µL	12.5 µL	37.5 µL	X
	G	X	-	50 µL	50 µL	25 µL	50 µL	X
	H	X	X	X	X	X	X	X

Note. Numerical values represent volume of 80 µM curcumin working solution added to designated wells in accordance to table 1.

Table 4

Cisplatin Dosing of 96-Well Plates

	Column Number							
Row		1	2, 3	4 , 5	6, 7	8, 9	10, 11	12
	A	X	X	X	X	X	X	X
	B	X	-	-	2 µL	-	-	X
	C	X	-	-	2 µL	-	-	X
	D	X	2 µL	-	-	-	-	X
	E	X	3 µL	-	-	-	-	X
	F	X	-	-	-	-	-	X
	G	X	-	-	-	-	-	X
	H	X	X	X	X	X	X	X

Note. Numerical values represent volume of 0.2 mg/mL cisplatin working solution added to designated wells in accordance to table 1. A total of 4 wells were incorporated for combinations of cisplatin-curcumin (B6 and B7) and cisplatin-niclosamide (C6 and C7) to be tested.

Where necessary, growth medium was used to balance wells so final volume of each well reached 200 µL (see table 5). The plate was visually inspected for discrepancies once all pipetting was completed. While not depicted in table 5, the outer wells also received an additional 100 µL medium, raising their levels to 200 µL. Doing so allowed for the volume of outer wells to be compared to central wells when monitoring for signs of evaporation cause by the edge effect. The plate was then returned to the incubator for 48 hours.

Table 5

Balancing Volumes of 96-Well Plates Using Growth Medium

		Column Number						
Row		1	2, 3	4 , 5	6, 7	8, 9	10, 11	12
	A	X	X	X	X	X	X	X
	B	X	100 µL	75 µL	60.5 µL	77.5 µL	37.5 µL	X
	C	X	100 µL	50 µL	73 µL	65 µL	25 µL	X
	D	X	98 µL	87.5 µL	82.5 µL	52.5 µL	37.5 µL	X
	E	X	97 µL	75 µL	70 µL	40 µL	25 µL	X
	F	X	95 µL	62.5 µL	57.5 µL	62.5 µL	12.5 µL	X
	G	X	90 µL	50 µL	45 µL	50 µL	-	X
	H	X	X	X	X	X	X	X

Note. The curcumin, niclosamide, and cisplatin concentrations depicted in table 1 will be realized once all wells are balanced at 200 µL total volume.

alamarBlue Cell Viability Reagent™ Assay

ThermoFisher Scientific's alamarBlue Cell Viability Reagent™ was used in combination with Thermo Scientific's Fluroskan Ascent microplate reader to collect data from the curcumin-niclosamide combination study. This assay works by introducing the resazurin-based product, blue in color, to a culture of cells. In the culture, resazurin can permeate living, metabolically active cells possessing reductive cytosol necessary to convert resazurin to resorufin, a red fluorescent compound (alamarBlue, n.d.). After alamarBlue was added, the Fluroskan device was used to collect readings at time internals. The numbers generated were proportional to the level of fluorescent signal being produced by resorufin. Wells containing either the most viable or greatest number of surviving cells showed the greatest amount fluorescence.

A 96-well plate that has been seeded at t = 0 hours, drugs-phytochemicals added at t = 24 hours, and has been allocated time to grow will undergo this assay beginning at t = 72 hours. At this time, aliquots of alamarBlue equaling 10% original volume of the well, i.e. 20 μL, were added to all 60 central wells intended for data collection. The plate was then scanned immediately after the final well received its portion of alamarBlue.

The plate reader software settings were customized based on the Costar (3596) 96-well plates. A second modification included a 10 second shaking stage set at 60 RPM was indented to ensure even distribution of alamarBlue and the converted product. Settings for excitation and emission were 544nm and 590nm, respectively.

The first scan conduced immediately after alamarBlue was added to the well plate served as zero hour for data collection. Plates would then be scanned every hour over a 4 hour period as was recommended for this type of study (alamarBlue, n.d.). In between scans, the well plate was placed back into the incubator to prevent light from interfering with alamarBlue's stability (alamarBlue, n.d.). Data readouts from scanning were provided in an excel-style table. The data generated from each plate was recorded along with unique plate identifying information, e.g. date of experiment, plate number, time of scan, etc.

Transfection of SKOV3 Cells with Autobioluminescence PB-lux Cassette

SKOV3 ovarian cancer cells were transfected with three plasmids to establish an autobioluminescent cell line intended for future use in imaging. The first plasmid, PB-lux, was created through ligation. $pCMV_{LUX}$ containing a cytomegalovirus promoter for a luciferase gene cassette (490 BioTech) was ligated to PB-RN, a

piggyBac transposon containing neomycin resistance (provided courtesy of Dr. Kelvin Kwan). Avery Lee, a former honors research student in Dr. Dunne Fong's laboratory, performed the ligation used to create the PB-lux plasmid. PB-lux would serve as the source of bioluminescence by coding for both the enzyme, luciferase, and substrate, luciferin, required for signaling (Close, 2012). If only a luciferase gene was introduced then researchers would have to inject substrate for signaling to occur. Hence, autobioluminescence refers to the cells' ability to perform the entire process on their own. Cells expressing autobioluminescent would allow for monitoring of tumor progression by observing the signal strength produced when imaging *in vivo* models.

The second and third plasmids used in transfection were AAT-PB-CD2APtk (Addgene) and pRP-hyPBase-mcherry (Vector Builder product provided courtesy of Dr. Arash Hatefi). The AAT-PB-CD2APtk plasmid (hereon referred to as AAT) contained genes for DsRed and puromycin resistance. Red fluorescent protein (RFP) signal produced by DsRed's gene product was useful in preliminary checks for successful transfection. Puromycin resistance was necessary for the selection process that followed. The third plasmid, pRP-hyPBase-mcherry (referred to as PBase), was part of the piggyBac system (Vector Builder, n.d.). PBase was the transposase complementing PB-lux in an effort to achieve stable expression of the luciferase cassette. The PBase plasmid also contained a gene for mCherry, an RFP derivative of DsRed, which also contributed to fluorescence imaging. Plasmid maps for CMV_{LUX}, AAT, and PBase are represented in supplemental figures 1, 2, and 3.

The transfection was performed using Invitrogen's lipofectamine 3000. Steps for the procedure followed guidance provided in the manufacturer's instruction manual with modifications made to suit the experiment. A Costar 6-well treated plate filled

with 3 mL medium per well was seeded with 300,000 cells per well 24 hours prior to transfection. At time of transfection, the wells were drained and replaced with 2mL medium. Two 1.5 mL centrifuge tubes were used to prepare the Lipofectamine mixtures. Both tubes received 125 μL Opti-MEM. Furthermore, Tube A received 3.5 μL of lipofectamine 3000 reagent before vortexing for 2 seconds (Invitrogen, n.d.). Tube B received 3 μL of P3000 reagent along with PB-lux, AAT, and PBase before mixing (Invitrogen, n.d.). The three plasmids were incorporated as an 8 to 1 to 1 ratio, respectively. Contents of tube A were added to tube B, mixed by pipetting, left to incubate for 15 minutes at room temperature, and finally added dropwise to one well from the overnight 6-well plate (Invitrogen, n.d.).

The cells were checked for RFP signals using a fluorescence microscope 48 hours after transfection. Positive RFP signals marked the beginning of puromycin selection. The RFP positive well was passaged with cells subcultured into another 6-well plate with two wells receiving $1/4^{th}$, two well receiving $1/8^{th}$, and two well receiving $1/16^{th}$ of the resuspended cell pellet. Volume of the wells were maintained at 4 mL with 5 μg/mL of puromycin being added to the medium (Adipogen, n.d.). Medium was removed, wells washed, and puromycin containing medium replaced regularly.

All wells were passaged on the 12^{th} day after transfection. Half of the collected cells were frozen in the event an error transpired during antibiotic selection. The concentration of remaining cells was counted using a hemocytometer followed by a portion being diluted in puromycin containing growth medium. The dilution resulted in a concentration of 1 cell per 10 μL. This 10 μL cell stock was added to a 96-well treated plated containing 90 μL of puromycin medium per well. An additional 6-well plate, receiving 15 cells per well, was also prepared for the selection process. The volume of these wells was maintained at 4 mL of puromycin medium.

Inspections of the wells were conducted regularly. A written record was used to document the wells that contained cells as well as how many clones appeared per well. Due to the small surface area of 96-well plates, well containing more than 1 clone were discarded. Clones developing in 6-well plates were monitored to prevent clusters from merging. Clones from both plates would later be transferred to Costar 12-well treated plates once they had developed to the point of being seen by eye.

Prior to starting the clone transfer process, 12-well plates containing 2 mL puromycin growth medium were prepared. The objective was to transfer 1 clone into its new well without risking the uptake of cells from a different clone. Transfer of clones was performed methodically as to not allow cultures to dry out or become over trypsinized.

All well of the 96-well plate were drained of medium. This was not only intended to prepare the single clone wells for washing, but also to prevent splashing during the trypsinization stage from wells that were not intended to be used during the transfer. Wells were washed with 100 μL of saline. Delivery of 20 μL of trypsin, a 1 minute incubation period, and tapping of the plate were used to release of cells from the monolayer. Addition of 100 μL of puromycin growth medium to each well was used to neutralize the trypsin. The contents of the well were pipetted up and down once before transfer to waiting 12-well plates.

The 6-well plates containing approximately 15 clones per well underwent a different transfer process. The plate was drained of medium before receiving a 1 mL saline wash. Each well received 200 μL of trypsin to coat the entire surface area. The trypsin was removed immediately, and the plate was incubated for 15 seconds. The modification here allowed for residual trypsin to perform its function, but to a lesser

degree. It was thought that the reduced effect and overall volume of trypsin would act to prevent separate clones from migrating to adjacent areas where unintentional uptake of 2 clones may occur. A pipette loaded with 10 μL of medium was brought into contact with a clone so that rapid, short cycles of pipetting could be used to uptake cells. The captured clone was then transferred to its location in a new 12-well plate.

When transferring clones, the lid of the 6-well plate was placed underneath one side of the plate in order to prop it at a slight angle. Clones nearest the bottom (6 o'clock) position of the well were transferred first. Progress was made working towards the top of the well. Having the 6-well plate held at an angled allowed excess medium to run down the plate instead of spreading outward towards adjacent clones. By transferring clones near the bottom of the well first, medium running down the plate would only pass over regions where clones had already been collected. Furthermore, critical attention was paid to prevent cross contaminate of clones during this process. If any doubt of a possible crossover existed then the offending cultures were discarded.

The 12-well plates containing 1 clone per well were given time to grow as medium was maintained at 5 μg/mL puromycin. Once the wells were about 50% confluent a fluorescent microscope was used to ensure clones still expressed RFP. When majority of the wells reach 80% confluence it was decided all wells would be passaged. Cells were collected into 1.5 mL tubes, centrifuged, and resuspended in 200 μL of medium. A black walled, clear bottom Falcon 96-well treated plate was prepared by adding 50 μL of medium per well based on the number of clones (45) maintained. A 50 μL portion from each 1.5 mL microcentrifuge tube was added to a partially filled well on the Falcon plate. The remaining cells were kept on ice.

Imaging for autobioluminescence was performed at Rutgers Molecular Imaging Center. Scans were accomplished using Bruker's In-Vivo MS FX PRO. Positive results showing autobioluminescence were noted so that corresponding samples left at our laboratory could be divided into portions meant for both expansion and storage.

Results

Curcumin and Niclosamide Combination Study

Eight 96-well plates were ran according to the study design. Two plates were prepared per week to reduce the chance of experiencing biases associated with cell culture conditions. The alamarBlue assay and Fluroskan plate reader allowed quantitative data to be collected as an Excel file. Data analysis began by determining the averages of control and experimental groups based on the alamarBlue readings recorded at hour 4 of the assay (see supplemental table 1). It was noticed that outer wells containing medium with no addition of alamarBlue produced a reading near zero. However, the blank control (one of the central 60 wells to receive alamarBlue) did produce a baseline reading. The average for the blank control was subtracted from all other calculated averages. Doing so removed the background signal caused by alamarBlue (see supplemental table 1).

Next, the untreated control well was used to determine viability of the different treatment groups. This calculation was performed using the average of each control or experimental group and dividing those numbers by the average value of the untreated control. Resulting values were multiplied by 100 to yield percentages. The data from these calculations would become the percentages of cell viability .

In figure 2, cell viabilities of control groups were compared to those of combination therapies. T-tests were performed between various groups to determine if a real difference existed in the data collected. Controls for 2.5 μM niclosamide and 15 μM curcumin returned $P \leq 0.001$ values when compared to their combination. Statistical significances between cell viabilities was also confirmed when 2 μg/mL cisplatin and 15 μM curcumin controls were matched against data obtained from their

combined treatment. Similar results were discovered when observing the effects of 2 µg/mL cisplatin and 2.5 µM niclosamide controls against their combination therapy.

Figure 2

alamarBlue Assay Results

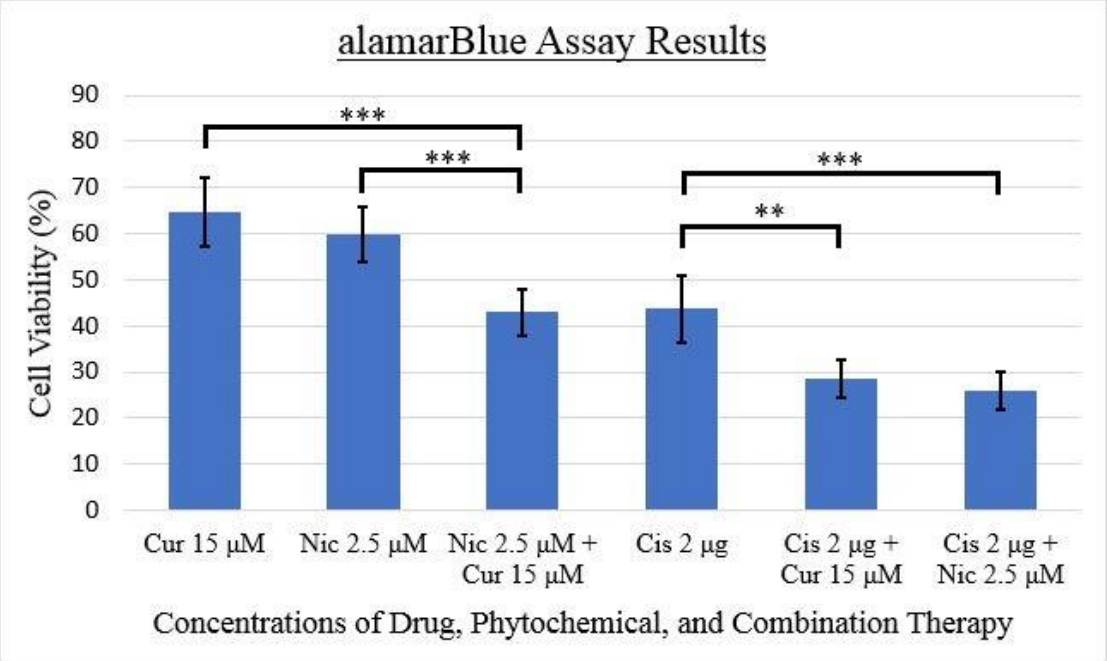

Note. Experimental groups were compared to their controls. Confidence intervals were set at 95%. T-tests were used to determine significance between groups. Significance levels followed the standards of The New England Journal of Medicine. Here, ** indicates $P \leq 0.01$ and *** indicates $P \leq 0.001$. Not shown in figure 2 is the t-test results comparing 15 µM curcumin against 2 µg/mL cisplatin + 15 µM curcumin. Also absent from the figure is the comparison of 2.5 µM niclosamide against 2 µg/mL cisplatin + 2.5 µM niclosamide. In both cases $P \leq 0.001$.

Curcumin-niclosamide treatment groups were investigated for synergistic qualities by a computer program called CompuSyn. The software utilizes control and experimental data from combination studies to generate detailed information on synergism, dose reductions, projected dose-effect levels, and many other statistics (Chou, 2005). CompuSyn employs calculations developed by Dr. Ting-Chao Chou and Dr. Paul Talalay, including the combination index equation, to aid in the determination of synergism (Chou, 2010). Data interpretation by the software yields combination index (CI) values where CI<1 indicates synergism, CI=1 is an additive effect, and CI>1 represents antagonism caused by drug mixtures (Chou, 2010).

Analysis by CompuSyn returned CI values for the 16 curcumin-niclosamide combinations tested (see table 6). Of the combinations tested, 8 were determined to be synergistic, 5 were antagonistic and 3 worked in an additive manner. Synergistic groups consisted of intermediate levels (1 μM and 2.5 μM) of niclosamide. It was found that the high (5 μM) and low (0.5 μM) dosages of niclosamide were characteristic of antagonists.

Table 6

Synergistic Properties of Curcumin-Niclosamide Combinations on SKOV3 Cells

Niclosamide Dosage	Curcumin Dosage	Combination Index (CI)	Level of Synergism
0.5 µM	5 µM	0.96	Nearly additive
0.5 µM	10 µM	1.17	Slight antagonism
0.5 µM	15 µM	1.06	Nearly additive
0.5 µM	20 µM	0.78	Moderate synergism
1 µM	5 µM	0.74	Moderate synergism
1 µM	10 µM	0.86	Slight synergism
1 µM	15 µM	0.81	Moderate synergism
1 µM	20 µM	0.74	Moderate synergism
2.5 µM	5 µM	0.87	Slight synergism
2.5 µM	10 µM	0.91	Nearly additive
2.5 µM	15 µM	0.86	Slight synergism
2.5 µM	20 µM	0.83	Moderate synergism
5 µM	5 µM	1.18	Slight antagonism
5 µM	10 µM	1.13	Slight antagonism
5 µM	15 µM	1.24	Moderate antagonism
5 µM	20 µM	1.17	Slight antagonism

Note. Combination index (CI) values for the 16 curcumin-niclosamide variants tested. The characteristic of synergism or antagonism was defined by CI ranges: <0.1 very strong synergism, 0.1-0.3 strong synergism, 0.3-0.7 synergism, 0.7-0.85 moderate synergism, 0.85-0.90 slight synergism, 0.90-1.10 nearly additive, 1.10-1.20 slight antagonism, 1.20-1.45 moderate antagonism, 1.45-3.3 antagonism, 3.3-10 strong antagonism, and >10 very strong antagonism (Chou, 2005)(Chou, 2006).

Even though other concentrations of curcumin-niclosamide performed at the level of being moderately synergistic, 1 µM niclosamide and 5 µM curcumin was chosen as a focal point for discussion. The key decision factor leading to this choice was the reduced concentration of curcumin. Despite using the lowest concentration of

curcumin and second lowest for niclosamide, the mixture produced the greatest level of synergism among all groups. Comparisons between the 1 μM niclosamide and 5 μM curcumin combination therapy and independent controls of equal strength are depicted in figure 3. T-tests were used to confirm statistical differences exist between controls and the experimental group.

Figure 3

Synergism of Niclosamide and Curcumin

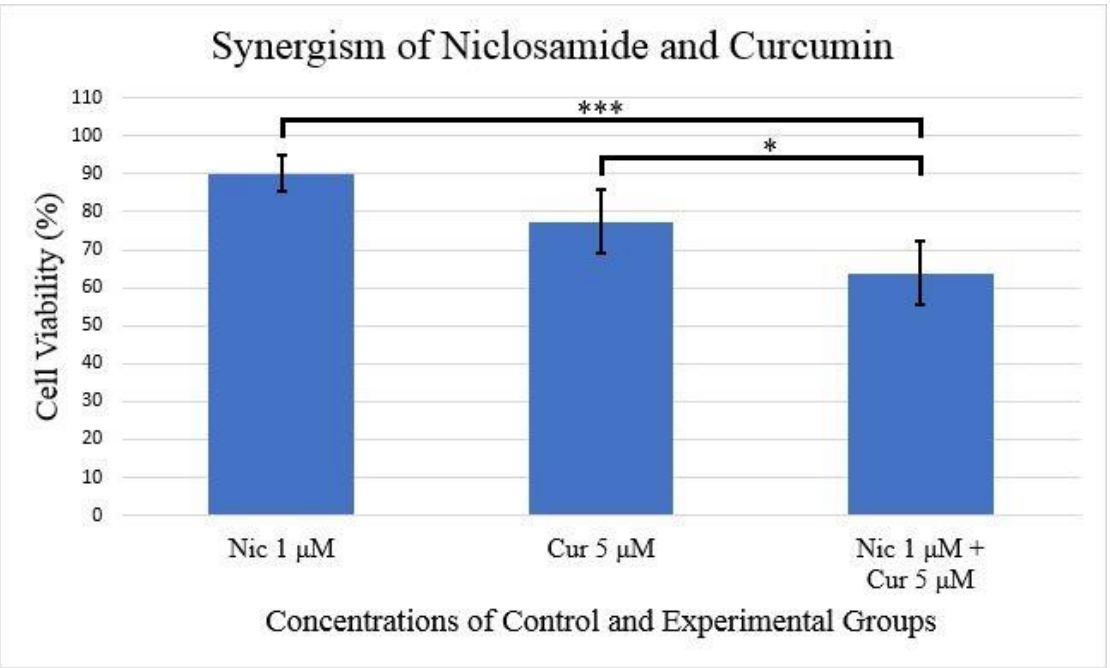

Note. The Chou-Talalay method for determining synergistic relationships indicated that 1 μM niclosamide combined with 5 μM curcumin possessed a moderate level of synergism (see table 6). T-tests comparing controls to the drug combination group show a significant difference exists. Confidence intervals were set at 95%. Significance levels followed the standards of The New England Journal of Medicine. Here, * indicates $P \leq 0.05$ and *** indicates $P \leq 0.001$.

Establishment of SKOV3 Autobioluminescent Cell Line

SKOV3 ovarian cancer cells were used to create an autobioluminescent cell line expressing a luciferase gene cassette. Following transfection with PB-lux, AAT and PBase via lipofectamine 3000, cells contained in 6-well plates were taken to the W.M. Keck Center for Collaborative Neuroscience where they would be inspected for fluorescence. Imaging the plate 48 hours post transfection was done to confirm the lipofectamine procedure was successful before carrying on with puromycin selection.

Figure 4 shows positive signals detected for RFP produced by the presence of AAT and PBase plasmids. Due to this image being taken only 48 hours post transfection, it is possible that the signal was caused by transient expression. At this point in time we could not be certain that cells positive for RFP had in fact been successfully transfected with the PB-lux plasmid for autobioluminescence. As such, selection had to be carried out to increase the likelihood of finding a PB-lux positive cell.

Figure 4

Cells Expressing RFP 48 Hours Post Transfection

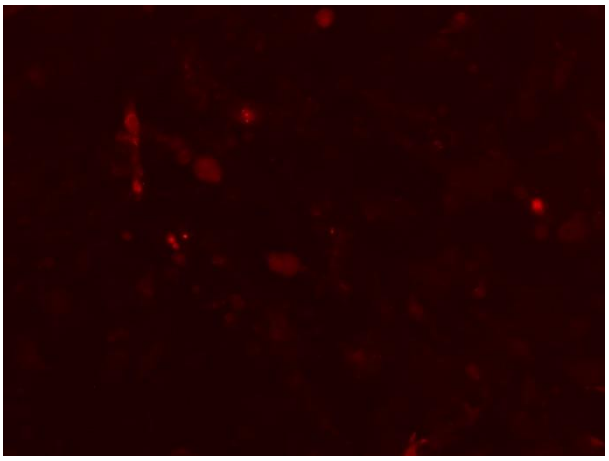

Note. Fluorescent imaging of 6-well plates showed transfection was successful to the point that RFP was being expressed either transiently or by stable expression. Image was taken under 200x total magnification.

Once clones had been transferred to 12-well plates and these wells reached approximately 80% confluences, they were checked again for RFP strength. The clones were then transferred to a special black walled plate designed to prevent interference from adjacent wells while imaging. This plate was taken to Rutgers Molecular Imaging Center where testing for autobioluminescence could be conducted. At the imaging center, the MS FX PRO was used to collect autobioluminescent signal over the course of 20 minutes. The readings were compiled and laid over an image of the well plate to form a heat map used to identify the location of positive clones and the strength of their signal (see figure 5).

Figure 5

Confirmation of Autobioluminescence Through PB-lux Expression by Clone

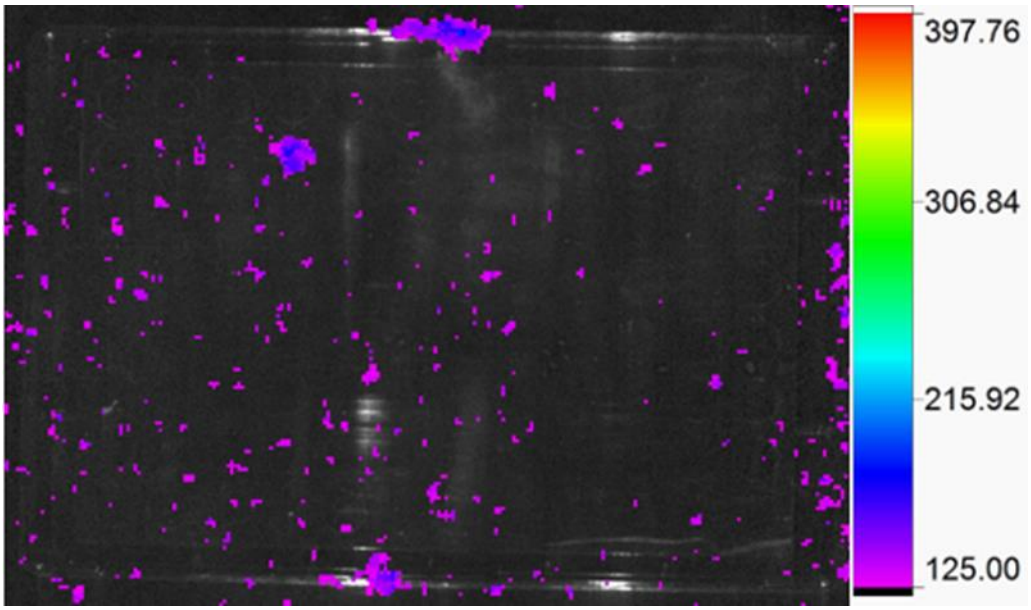

Note. The MS FX PRO was used to identify one positive clone through a 20 minute scan of the Falcon 96-well plate. Well B4 was determined to be a real signal. Signals detected at the 6 and 12 o'clock positions were considered to be artifacts caused by the plate.

The positive clone in well B4 was named SKOV3a8 based on the clone's transfection origin. Two different flasks of SKOV3a8 were subcultured from well B4, one in ordinary growth medium and the second in growth medium containing 5 µg/mL puromycin. These two cultures were grown for 1 week before being tested a second time to quantify signal strength based on a known concentration of cells.

Figure 6 was captured 1 week after figure 5 was taken. The follow-up image was conducted to determine the number of SKOV3a8 cells required to produce a detectable signal. It was determined that 25,000 and 50,000 cells were not enough to

produce a reliable image. The wells containing 100,000 cells did produce a reliable autobioluminescence signal. Figure 6 revealed a second positive clone in well B10. When inspecting figure 5, it appears that a week signal may have been detected in the center of well B10.

Figure 6

Evaluation of Autobioluminescence Strength with MS FX PRO

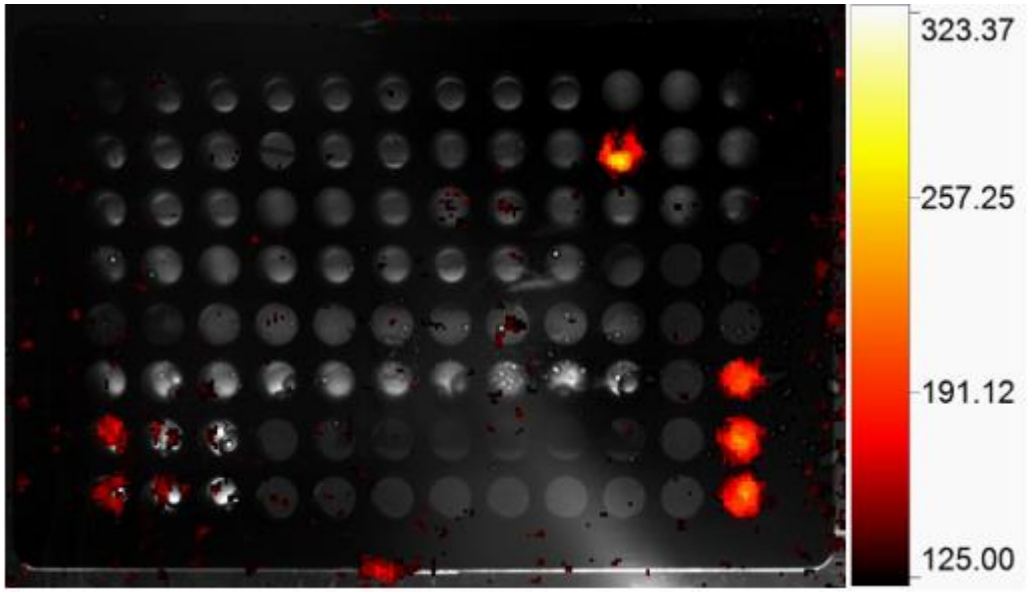

Note. This image is of the same plate shown in figure 3 taken 1 week later. A new positive clone appeared in well B10. The positive signal from well B4 is not present in figure 6 due to passaging of this well. SKOV3a8 cells maintained in 5 μg/mL puromycin were plated in wells G1, G2, and G3 with 100,000, 50,000, and 25,000 cells, respectively. SKOV3a8 cells absent of puromycin selection were placed in wells H1, H2, and H3 with 100,000, 50,000, and 25,000 cells, respectively. The right most signals were built in as a failsafe in the event 100,000 cells did not produce a noticeable signal. Wells F12 and G12 received 1/5th the pelleted cells obtained from

an 80% confluent SKOV3a8 flask grown in the presence of puromycin. Well H12 received 1/5th the pelleted cells obtained from an 80% confluent SKOV3a8 flask grown in the absence of puromycin. Hints of the artifacts seen in figure 5 were also present at the 6 and 12 o'clock positions.

Discussion

Statistical analysis of data supported the notion that a real, favorable difference existed when phytochemicals and repurposed FDA approved drugs were used in combination as opposed to their independent use in targeting ovarian cancer cells. Figure 2 provides evidence that this is indeed the case when 2.5 μM niclosamide is used alongside 15 μM curcumin in disrupting SKOV3 cell viability. Data collected for 2 μg/mL cisplatin combined with 15 μM curcumin further supports this concept. The decreased cell viability caused by the union of cisplatin and curcumin complements with the findings of Yallapu's study displayed in figure 1. Visual inspections of the 96-well plates 48 hours post drug delivery, the same timing as Yallapu, found cell cultures appearing in a similar state as those photographed in figure 1. Closely matching the results of cisplatin-curcumin combination treatment acts to add credibility to the overall study design and findings.

Even though some treatment wells appeared to have a lower cell count 48 hours after compounds were added, it must be noted that an alamarBlue assay alone does not reveal the underlying mechanism responsible for the differing cell viability values. The cause of lower cell viabilities may be due to cell death, inhibition of proliferation, or decreased metabolic activity of cells. An additional alamarBlue assay conducted immediately upon seeding 3000 cells would provide a bit more insight. Knowing the signal value for 3000 cells would provide a reference point to compare against the treatment group signals collected after the experiment. While not definitive, it would help to gauge what wells have continued proliferation. Counting of the number of cells per well is an option that would determine if cell death did occur.

The goal to discover synergistic relationships between curcumin and niclosamide was achieved in 8 successful pairings. The combinations to show the most synergism included intermediate levels (1 μM and 2.5 μM) of niclosamide whereas the flanking extremes (0.5 μM and 5 μM) were contributors to antagonistic effects. A pattern explaining curcumin's influence was more difficult to identify. An expanded study where 1 μM and 2.5 μM niclosamide are used in combination with a wider range of curcumin concentrations may help to gather more evidence to discern curcumin's contribution to the synergistic nature of the two molecules.

Focusing on the mixture of 1 μM niclosamide and 5 μM curcumin highlighted the potential that exists for these two compounds in cancer treatment. These low concentration doses produced the highest level of synergism among the 16 variants. Generally, when drugs are being designed and tested there exists a goal to have the greatest beneficial effect of the drug while administering the lowest dose possible. This acts to reduce the likelihood and severity of adverse effects while also keeping production costs down for the manufacturer.

The study may benefit from slight adjustments, e.g. drug concentrations, that may yield even better results when it comes to reducing cell viability. However, the schedule of allowing seeded cells a portion of time to grow before addition of drug molecules should be kept. If niclosamide, curcumin, or cisplatin were added to wells at the same time as seeding then data would most likely reflect misleading results. Providing cells with time to attach to the plate and return to a more natural morphology, through contacting another surface, helps to create a better test environment despite being an *in vitro* study. If single cells were in suspension at the time drugs and phytochemicals were added then attachment required for monolayer formation may be inhibited. A difference would also exist in the percentage of surface

area exposed to the drugs when considering single cells in suspension vs attachment. The duration of 48 hours of cells exposure to drug molecules seems to be a common time frame used in research. Therefore, extending the exposure period is not an approach that would be recommended.

Creation of an autobioluminescent cell line using SKOV3 cells was a lengthy process. A number of checkpoints were designed to confirm the project was kept on track and to reduce risks of errors or unforeseen events. The lipofectamine 3000 transfection procedure was followed up by fluorescence imaging of cells to confirm the presence of RFP production. The positive signal indicated puromycin selection should begin in order to find cells with stable expression of the plasmids.

Samples of the transfected cells were frozen for long term storage as a precaution upon entering the selection process. After puromycin selection and the expansion of clones, samples were able to be inspected for autobioluminescence using the MS FX PRO. The positive clone (SKOV3a8) from well B4 in figure 5 was passaged from the plate. A portion of the collected cells were used for expansion with the rest being placed into storage. Two flasks were made from the SKOV3a8 cells: one containing 5 μg/mL puromycin and the other being antibiotic free.

A second scan of SKOV3a8 was conducted to see if expression remained after puromycin was removed from the culture medium and to determine the number of cells required to produce a reliable signal. In figure 6, wells in row G contained SKOV3a8 cells with continued puromycin selection. Wells from row H contained cells grown without puromycin. Equal concentrations of cells were plated according to column number. Figure 6 confirmed a real signal was produced by 100,000 cells suspended in 200 μL of medium (wells G1 and H1). With a weak signal being

produced by 50,000 cells (wells G2 and H2), it reasonable to suggest a reliable signal could be detected within the range of 50,000 to 100,000 cells with confirmation provided by a future test. Comparing the strength of signals produced in row G to that of row H shows nearly identical values between the two cultures. This suggests the luciferase cassette is being express stably in both puromycin and antibiotic free cultures.

A surprise outcome occurred when a second positive autobioluminescent clone was detected in well B10 of figure 6. Instinctively, figure 5 was checked for indications of a signal from the prior week. There seems to be a very weak signal at the center of well B10 in figure 5, but it was overlooked at the time since it did not stand out from background readings. The missed detection during earlier imaging may have been caused by a low cell concentration. Counting and seeding 45 clones during the first autobioluminescence test was deemed impractical as there were uncertainties with the number of cells required to produce a signal and if a positive clone even existed. The follow up scan performed 1 week later was designed to compensate for this shortcoming.

Future plans for the SKOV3a8 autobioluminescent cell line involve an *in vivo* study using immunodeficient mice. An animal protocol has been submitted to Rutgers University's Institutional Animal Care and Use Committee (IACUC) with negotiation currently underway. The animal study proposes the use of curcumin and niclosamide in the treatment of mice exhibiting tumors derived from ovarian cancer cell injections. It was decided that subcutaneous and intraperitoneal delivery would be used as the two study groups with various control and experimental cohorts for each. The decision for the two groups stem from the desire to use the autobioluminescent cell line for imaging. The ability of SKOV3a8 cells to produce a signal without the need

for substate inject benefits animal studies by reducing the number of invasive procedures needed.

Having a well-rounded understanding of both cancer biology and available treatment options allows for a greater chance at discovering new methods useful in cancer care. The combination therapy approach acts to boost the efficacy of first line treatments. Providing chemotherapeutics to a patient following a surgical procedure to remove late stage or aggressive forms of cancers is a common strategy already in place. A more refined approach would be to develop and deploy novel therapeutic agents designed to target persistent subpopulations of cancer cells that fit the cancer stem cell model. New treatments that target resistant cells will also benefit patients who have tumors exhibiting resistance to prior medications. Reducing the number of relapse events by targeting cancer stem cells during first line treatment is also a way to reduce the cost burden of cancer.

However, companies capable of financing clinical trials cannot be easily persuaded to invest in phytochemical research. The issue stems from intellectual property laws preventing naturally occurring molecules from being patented. Companies require some form of exclusivity as a means to recuperate their development costs. The best known case pertaining to this subject is Taxol (paclitaxel). The popular anticancer drug was found in the bark of the pacific yew, researched by the National Cancer Institute, and commercialized by Bristol-Myers Squibb under a 5-year exclusivity deal instead of a typical 20 year patent (Garber, 2002). While Bristol-Myers Squibb did profit from the deal, the legal troubles surrounding the case were complex to say the least. The most likely way of seeing phytochemical-repurposed drugs combinations reach the market is through companies combining it with their own proprietary drugs. Companies may be persuaded if

evidence is presented that curcumin-niclosamide dosing increases sensitivity of cancer cells to their proprietary drug, causing an increase in efficacy. This concept would align with the results observed between cisplatin and curcumin.

With all things considered, the solution to the problem that is cancer may not be a better drug, but a more effective first treatment. If therapies can be diverse enough to eliminate all cancer cells during the first line of treatment then the chance of relapses would be non-existent. Instead of an evasive cancer cell surviving to reform a tumor, a separate mutagenic event would have to occur. Of course, this is easier said than done. However, if therapies can target a few prevalent subpopulations of tumor cells then the rate of relapse can be diminished.

The results obtained from curcumin and niclosamide provide some interesting possibilities for a new treatment that could benefit people on both sides of the financial spectrum. Those with the means to receive quality treatment will have an additional option that can be called upon and those with little or no financial security may see the appearance of a treatment option for a disease that would otherwise go uncared for. In the end, if a war chest of cancer drugs with different molecular targets can be assembled then patients will have a better opportunity at reaching a favorable outcome.

References

1. Addgene: AAT-PB-CD2APtk (Plasmid #86004). (n.d.). Retrieved from https://www.addgene.org/86004/
2. Adipogen Life Science. (n.d.). Retrieved April 10, 2020, from https://adipogen.com/ag-cn2-0078-puromycin-dihydrochloride.html
3. alamarBlue™ Cell Viability Reagent. (n.d.). Retrieved April 3, 2020, from https://www.thermofisher.com/order/catalog/product/DAL1100#/DAL1100).
4. Bercow, A. S., Chen, L., Chatterjee, S., Tergas, A. I., Hou, J. Y., Burke, W. M., … Wright, J. D. (2017). Cost of Care for the Initial Management of Ovarian Cancer. *Obstetrics & Gynecology*, *130*(6), 1269–1275. doi: 10.1097/aog.0000000000002317
5. BRCA Mutations: Cancer Risk and Genetic Testing Fact Sheet. (n.d.). Retrieved December 4, 2017, from https://www.cancer.gov/about-cancer/causes-prevention/genetics/brca-fact-sheet#q1
6. Chan, M. M., Fong, D., Soprano, K. J., Holmes, W. F., & Heverling, H. (2002). Inhibition of growth and sensitization to cisplatin-mediated killing of ovarian cancer cells by polyphenolic chemopreventive agents. *Journal of Cellular Physiology*, *194*(1), 63–70. doi: 10.1002/jcp.10186
7. Chou, T.-C. (2006). Theoretical Basis, Experimental Design, and Computerized Simulation of Synergism and Antagonism in Drug Combination Studies. *Pharmacological Reviews*, *58*(3), 621–681. doi: 10.1124/pr.58.3.10
8. Chou TC. (2010). Drug combination studies and their synergy quantification using the Chou-Talalay method. *Cancer Res* 70: 440-446, 2010. “doi: 10.1158/0008-5472.CAN-09-1947”
9. Chou TC and Martin N. (2005). CompuSyn for Drug Combinations: PC Software and User’s Guide: A Computer Program for Quantitation of Synergism and Antagonism in Drug Combinations, and the Determination of IC_{50} and ED_{50} and LD_{50} Values, ComboSyn Inc, Paramus, (NJ), 2005.
10. Christophe, S., Cooper, A. L., Nelson, D. F., Doran, S., Ueland, F. R., DeSimone, C. P., … Jr, J. R. van N. (2009, January 31). Long-Term Survival and Cost of Treatment in Patients with Stage IIIC Epithelial Ovarian Cancer. Retrieved April 11, 2020, from http://www.eurekaselect.com/83887/article
11. Close, D., Xu, T., Smartt, A., Rogers, A., Crossley, R., Price, S., … Sayler, G. (2012). The Evolution of the Bacterial Luciferase Gene Cassette (lux) as a Real-Time Bioreporter. *Sensors*, *12*(1), 732–752. doi: 10.3390/s120100732
12. Curcumin. (n.d.). Retrieved April 11, 2020, from https://www.caymanchem.com/search?q=curcumin
13. Dasari, S., & Tchounwou, P. B. (2014). Cisplatin in cancer therapy: Molecular mechanisms of action. *European Journal of Pharmacology*, 740, 364-378. doi:10.1016/j.ejphar.2014.07.025
14. Du, H., & Taylor, H. S. (2009). Stem Cells and Female Reproduction. *Reproductive Sciences*, *16*(2), 126–139. doi: 10.1177/1933719108329956

15. Fong, D., & Chan, M. M. (2013). Mitochondria as Targets for Phytochemicals in Cancer Prevention and Therapy. New York, NY: Springer. doi: 10.1007/978-1-4614-9326-6
16. Fong, D., Yeh, A., Naftalovich, R., Choi, T. H., & Chan, M. M. (2010). Curcumin inhibits the side population (SP) phenotype of the rat C6 glioma cell line: Towards targeting of cancer stem cells with phytochemicals. *Cancer Letters*, *293*(1), 65–72. doi: 10.1016/j.canlet.2009.12.018
17. Garber, K. (2002). Battle Over Generic Taxol Concludes, But Controversy Continues. *CancerSpectrum Knowledge Environment*, *94*(5), 324–326. doi: 10.1093/jnci/94.5.324
18. Genentech About Avastin: Proposed Mechanism of Action. (n.d.). Retrieved December 1, 2017, from https://www.avastin.com/hcp/mcrc/proposed-moa.html
19. GRAS Notices. (2019, June 4). Retrieved March 29, 2020, from https://www.accessdata.fda.gov/scripts/fdcc/?set=GRASNotices
20. Hillen, F., & Griffioen, A. W. (2007). Tumour vascularization: sprouting angiogenesis and beyond. *Cancer and Metastasis Reviews*, *26*(3-4), 489–502. doi: 10.1007/s10555-007-9094-7
21. Invitrogen Lipofectamine 3000 protocol. (n.d.). Retrieved April 2, 2020, from https://www.thermofisher.com/document-connect/document-connect.html?url=https://assets.thermofisher.com/TFS-Assets/LSG/manuals/lipofectamine3000_protocol.pdf&title=TGlwb2ZlY3RhbWluZSAzMDAwIFJlYWdlbnQgUHJvdG9jb2wgKEVuZ2xpc2gp
22. Kozikowski, B. A., Burt, T. M., Tirey, D. A., Williams, L. E., Kuzmak, B. R., Stanton, D. T., … Nelson, S. L. (2003). The Effect of Freeze/Thaw Cycles on the Stability of Compounds in DMSO. *Journal of Biomolecular Screening*, *8*(2), 210–215. doi: 10.1177/1087057103252618
23. Li, Y., Li, P.-K., Roberts, M. J., Arend, R. C., Samant, R. S., & Buchsbaum, D. J. (2014). Multi-targeted therapy of cancer by niclosamide: A new application for an old drug. *Cancer Letters*, *349*(1), 8–14. doi: 10.1016/j.canlet.2014.04.003
24. Mackillop, W. J., Ciampi, A., Till, J. E., & Buick, R. N. (1983). A Stem Cell Model of Human Tumor Growth: Implications for Tumor Cell Clonogenic Assays2. *JNCI: Journal of the National Cancer Institute*. doi: 10.1093/jnci/70.1.9
25. Mendonsa, A. M., Na, T.-Y., & Gumbiner, B. M. (2018). E-cadherin in contact inhibition and cancer. *Oncogene*, *37*(35), 4769–4780. doi: 10.1038/s41388-018-0304-2
26. Mohandas KM, Desai DC: Epidemiology of digestive tract cancers in India. V. Large and small bowel. Indian J Gastroenterol 1999, 18:118-121.
27. Naksuriya, O., Steenbergen, M. J. V., Torano, J. S., Okonogi, S., & Hennink, W. E. (2016). A Kinetic Degradation Study of Curcumin in Its Free Form and Loaded in Polymeric Micelles. *The AAPS Journal*, *18*(3), 777–787. doi: 10.1208/s12248-015-9863-0
28. Neeley, C. (2016, July 7). Reducing the edge effect. Retrieved March 3, 2017, from https://www.thermofisher.com/blog/cellculture/reducing-the-edge-effect/

29. Niclosamide. (n.d.). Retrieved April 11, 2020, from https://www.caymanchem.com/search?q=niclosamide
30. Niclosamide (Oral Route) Description and Brand Names. (2020, February 1). Retrieved March 30, 2020, from https://www.mayoclinic.org/drugs-supplements/niclosamide-oral-route/description/drg-20065068
31. Odunsi, K., Matsuzaki, J., James, S. R., Mhawech-Fauceglia, P., Tsuji, T., Miller, A., … Karpf, A. R. (2014). Epigenetic Potentiation of NY-ESO-1 Vaccine Therapy in Human Ovarian Cancer. *Cancer Immunology Research*, *2*(1), 37–49. doi: 10.1158/2326-6066.cir-13-0126
32. Ovarian Cancer Statistics – Ovarian Cancer Research Alliance. (n.d.). Retrieved December 30, 2017, from https://ocrfa.org/patients/about-ovarian-cancer/statistics/
33. Ovarian Cancer Treatment: How to Treat Ovarian Cancer. (n.d.). Retrieved November 30, 2017, from https://www.cancer.org/cancer/ovarian-cancer/treating.html
34. Radiation Therapy. (n.d.). Retrieved March 31, 2020, from https://www.cancer.org/treatment/treatments-and-side-effects/treatment-types/radiation.html
35. Ramus, S. J., & Gayther, S. A. (2009). The Contribution of BRCA1 and BRCA2 to Ovarian Cancer. *Molecular Oncology*, *3*(2), 138–150. doi: 10.1016/j.molonc.2009.02.001
36. Rayfield, W. J., Kandula, S., Khan, H., & Tugcu, N. (2017). Impact of Freeze/Thaw Process on Drug Substance Storage of Therapeutics. *Journal of Pharmaceutical Sciences*, *106*(8), 1944–1951. doi: 10.1016/j.xphs.2017.03.019
37. Thomson, J. A., Itskovitz-Eldor, J., Shapiro, S. S., Waknitz, M. A., Swiergiel, J. J., Marshall, V. S., & Jones, J. M. (1998). Embryonic Stem Cell Lines Derived from Human Blastocysts. *Science*, *282*(5391), 1145–1147. doi: 10.1126/science.282.5391.1145
38. Vallianou, N. G., Evangelopoulos, A., Schizas, N., & Kazazis, C. (2015). Potential Anticancer Properties and Mechanisms of Action of Curcumin. *International Journal of Cancer Research and Treatment*, *35*(2), 645–651.
39. Vector Builder. (n.d.). Retrieved from https://v1.vectorbuilder.com/vector/VB160216-10057/?format=pdf&annotation_uuid=
40. Waters JC, Chen RH, Murray AW, Salmon ED J *Cell Biol*. 1998 Jun 1; 141(5):1181-91
41. Weaver, B. A. (2014). How Taxol/paclitaxel kills cancer cells. *Molecular Biology of the Cell*, 25(18), 2677-2681. doi:10.1091/mbc.e14-04-0916
42. Xu, T., Close, D., Price, S., & Sayler, G. (n.d.). High-Throughput Detection of Estrogenic Compounds Using ... Retrieved April 14, 2020, from https://490biotech.com/wp-content/uploads/2016/10/High-Throughput-Detection-490-BioTech.pdf

43. Yallapu, M. M., Maher, D. M., Sundram, V., Bell, M. C., Jaggi, M., & Chauhan, S. C. (2010). Curcumin induces chemo/radio-sensitization in ovarian cancer cells and curcumin nanoparticles inhibit ovarian cancer cell growth. *Journal of Ovarian Research, 3*(1), 11. doi:10.1186/1757-2215-3-11
44. Yo, Y.-T., Lin, Y.-W., Wang, Y.-C., Balch, C., Huang, R.-L., Chan, M. W. Y., … Lai, H.-C. (2012). Growth Inhibition of Ovarian Tumor-Initiating Cells by Niclosamide. *Molecular Cancer Therapeutics, 11*(8), 1703–1712. doi: 10.1158/1535-7163.mct-12-0002
45. Yoo, S., Kim, K., Nam, H., & Lee, D. (2018). Discovering Health Benefits of Phytochemicals with Integrated Analysis of the Molecular Network, Chemical Properties and Ethnopharmacological Evidence. *Nutrients, 10*(8), 1042. doi: 10.3390/nu10081042

Appendix

Supplemental Table 1

Average Readings for alamarBlue Assay

		Column Number						
		1	2, 3	4, 5	6, 7	8, 9	10, 11	12
Row	A	0.18	0.18	0.19	0.18	0.26	0.19	0.18
	B	0.18	24.67	342.36	175.76	363.30	252.59	0.18
	C	0.18	555.54	284.94	162.78	332.49	229.85	0.18
	D	0.18	256.43	436.23	418.72	291.46	270.24	0.18
	E	0.18	143.62	405.33	385.43	255.16	244.79	0.18
	F	0.18	522.67	368.33	339.50	309.23	243.19	0.18
	G	0.18	502.76	293.31	276.48	282.61	222.97	0.18
	H	0.18	0.19	0.18	0.19	0.18	0.18	0.18

Note. Readings follow the experimental design outlined in table 1. Edge wells containing medium did not receive alamarBlue. Wells B2 and B3 (blank controls) contained medium along with alamarBlue. The plate reader was tested with an empty well plate to see if the plastic itself contributed to low level readings. It was discovered that empty wells also produced a minuscule reading very similar to that of edge wells containing only medium. With no noticeable difference between empty wells and outer wells containing medium, it was concluded that alamarBlue (resazurin) was responsible for part of the fluorescent signal intended to detected levels of resorufin. If the impact of alamarBlue (24.67) was not subtracted from all other averages then errors would appear in data. For example, when determining cell viability, the value of blank wells should equate to zero. However, neglecting to subtract alamarBlue's impact on signaling would result in a 4.44% viability when dividing the blank well average by the untreated well average ([24.67/555.54]*100=4.44%). Clearly, a well absent of cells could not produce any level of cell viability. Thus, these corrective measures were implemented.

Supplemental Figure 1

CMV_{LUX} Plasmid Map

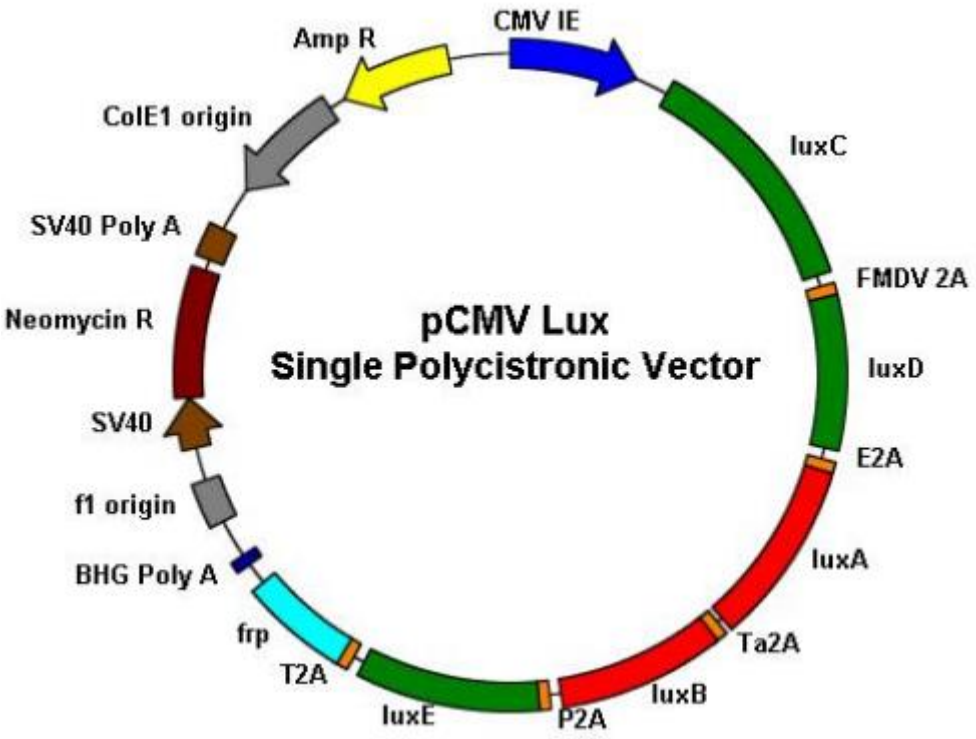

Note. Representation of the CMV_{LUX} plasmid used in creating SKOV3a8 autobioluminescent cells. Supplemental figure 1 was obtained from *High-Throughput Detection of Estrogenic Compounds Using Autonomously Bioluminescent Human Breast Cancer Cells* by Xu, n.d.

Supplemental Figure 2

AAT-PB-CD2APtk (AAT) Plasmid Map

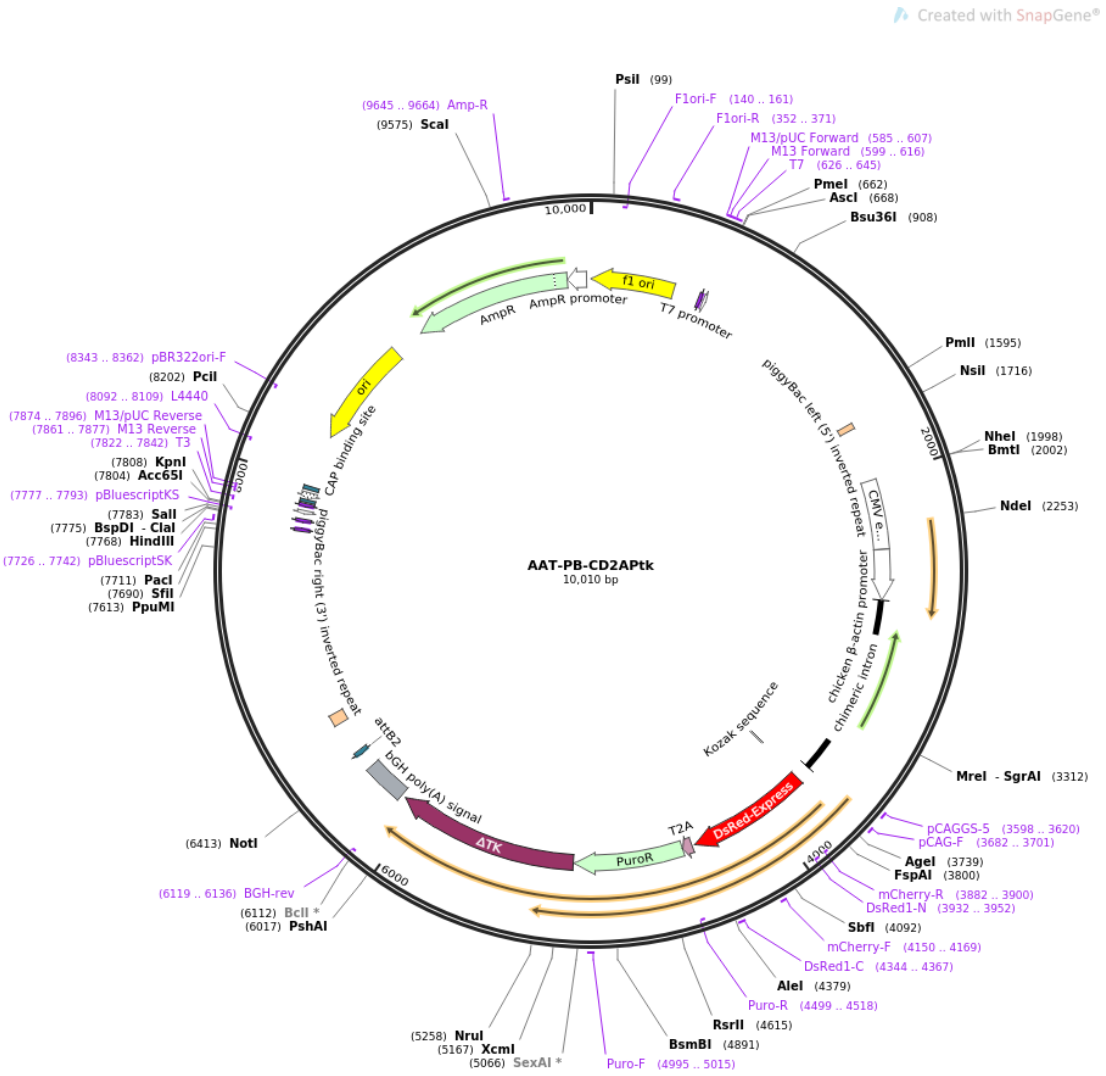

Note. Representation of the AAT plasmid used in creating SKOV3a8 autobioluminescent cells. Supplemental figure 2 was obtained from Addgene, n.d.

Supplemental Figure 3

pRP-hyPBase-mcherry (PBase) Plasmid Map

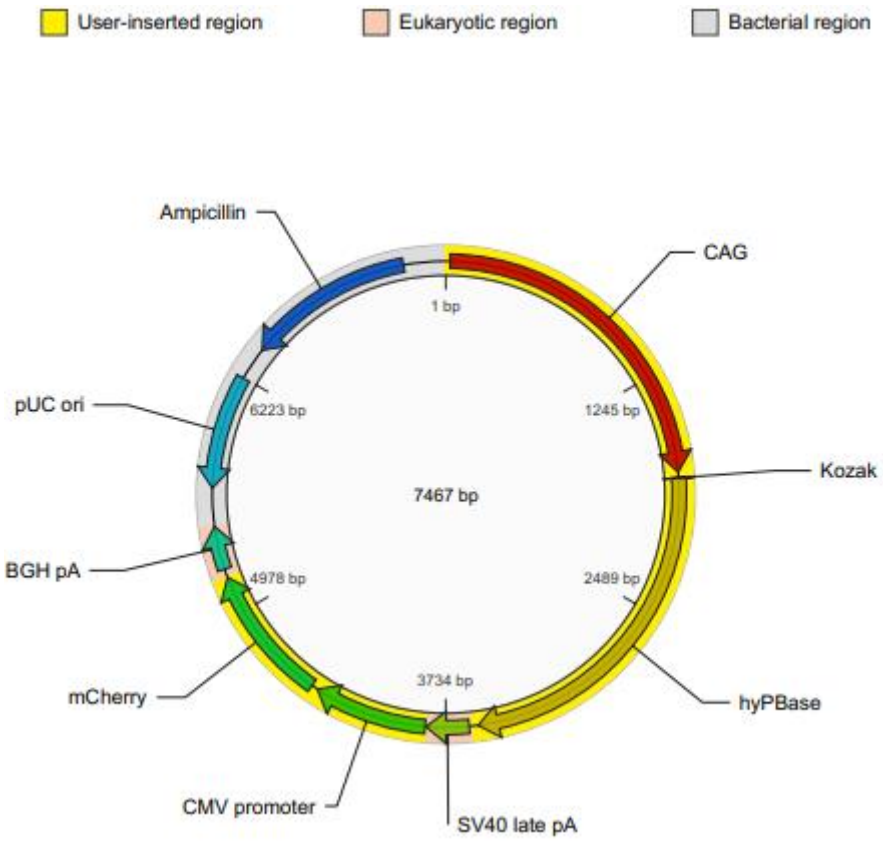

Note. Representation of the PBase plasmid used in creating SKOV3a8 autobioluminescent cells. Supplemental figure 3 was obtained from Vector Builder, n.d.

Bibliography

1. Addgene: AAT-PB-CD2APtk (Plasmid #86004). (n.d.). Retrieved from https://www.addgene.org/86004/
2. Adipogen Life Science. (n.d.). Retrieved April 10, 2020, from https://adipogen.com/ag-cn2-0078-puromycin-dihydrochloride.html
3. alamarBlue™ Cell Viability Reagent. (n.d.). Retrieved April 3, 2020, from https://www.thermofisher.com/order/catalog/product/DAL1100#/DAL1100).
4. Bercow, A. S., Chen, L., Chatterjee, S., Tergas, A. I., Hou, J. Y., Burke, W. M., … Wright, J. D. (2017). Cost of Care for the Initial Management of Ovarian Cancer. *Obstetrics & Gynecology*, *130*(6), 1269–1275. doi: 10.1097/aog.0000000000002317
5. BRCA Mutations: Cancer Risk and Genetic Testing Fact Sheet. (n.d.). Retrieved December 4, 2017, from https://www.cancer.gov/about-cancer/causes-prevention/genetics/brca-fact-sheet#q1
6. Chan, M. M., Fong, D., Soprano, K. J., Holmes, W. F., & Heverling, H. (2002). Inhibition of growth and sensitization to cisplatin-mediated killing of ovarian cancer cells by polyphenolic chemopreventive agents. Journal of Cellular Physiology, 194(1), 63–70. doi: 10.1002/jcp.10186
7. Chou, T.-C. (2006). Theoretical Basis, Experimental Design, and Computerized Simulation of Synergism and Antagonism in Drug Combination Studies. *Pharmacological Reviews*, *58*(3), 621–681. doi: 10.1124/pr.58.3.10
8. Chou TC. (2010). Drug combination studies and their synergy quantification using the Chou-Talalay method. *Cancer Res* 70: 440-446, 2010. “doi: 10.1158/0008-5472.CAN-09-1947”
9. Chou TC and Martin N. (2005). CompuSyn for Drug Combinations: PC Software and User’s Guide: A Computer Program for Quantitation of Synergism and Antagonism in Drug Combinations, and the Determination of IC_{50} and ED_{50} and LD_{50} Values, ComboSyn Inc, Paramus, (NJ), 2005.
10. Christophe, S., Cooper, A. L., Nelson, D. F., Doran, S., Ueland, F. R., DeSimone, C. P., … Jr, J. R. van N. (2009, January 31). Long-Term Survival and Cost of Treatment in Patients with Stage IIIC Epithelial Ovarian Cancer. Retrieved April 11, 2020, from http://www.eurekaselect.com/83887/article
11. Close, D., Xu, T., Smartt, A., Rogers, A., Crossley, R., Price, S., … Sayler, G. (2012). The Evolution of the Bacterial Luciferase Gene Cassette (lux) as a Real-Time Bioreporter. *Sensors*, *12*(1), 732–752. doi: 10.3390/s120100732
12. Curcumin. (n.d.). Retrieved April 11, 2020, from https://www.caymanchem.com/search?q=curcumin
13. Dasari, S., & Tchounwou, P. B. (2014). Cisplatin in cancer therapy: Molecular mechanisms of action. *European Journal of Pharmacology*, 740, 364-378. doi:10.1016/j.ejphar.2014.07.025
14. Du, H., & Taylor, H. S. (2009). Stem Cells and Female Reproduction. *Reproductive Sciences*, *16*(2), 126–139. doi: 10.1177/1933719108329956

15. Fong, D., & Chan, M. M. (2013). Mitochondria as Targets for Phytochemicals in Cancer Prevention and Therapy. New York, NY: Springer. doi: 10.1007/978-1-4614-9326-6
16. Fong, D., Yeh, A., Naftalovich, R., Choi, T. H., & Chan, M. M. (2010). Curcumin inhibits the side population (SP) phenotype of the rat C6 glioma cell line: Towards targeting of cancer stem cells with phytochemicals. *Cancer Letters*, *293*(1), 65–72. doi: 10.1016/j.canlet.2009.12.018
17. Garber, K. (2002). Battle Over Generic Taxol Concludes, But Controversy Continues. *CancerSpectrum Knowledge Environment*, *94*(5), 324–326. doi: 10.1093/jnci/94.5.324
18. Genentech About Avastin: Proposed Mechanism of Action. (n.d.). Retrieved December 1, 2017, from https://www.avastin.com/hcp/mcrc/proposed-moa.html
19. GRAS Notices. (2019, June 4). Retrieved March 29, 2020, from https://www.accessdata.fda.gov/scripts/fdcc/?set=GRASNotices
20. Hillen, F., & Griffioen, A. W. (2007). Tumour vascularization: sprouting angiogenesis and beyond. *Cancer and Metastasis Reviews*, *26*(3-4), 489–502. doi: 10.1007/s10555-007-9094-7
21. Invitrogen Lipofectamine 3000 protocol. (n.d.). Retrieved April 2, 2020, from https://www.thermofisher.com/document-connect/document-connect.html?url=https://assets.thermofisher.com/TFS-Assets/LSG/manuals/lipofectamine3000_protocol.pdf&title=TGlwb2ZlY3RhbWluZSAzMDAwIFJlYWdlbnQgUHJvdG9jb2wgKEVuZ2xpc2gp
22. Kozikowski, B. A., Burt, T. M., Tirey, D. A., Williams, L. E., Kuzmak, B. R., Stanton, D. T., … Nelson, S. L. (2003). The Effect of Freeze/Thaw Cycles on the Stability of Compounds in DMSO. *Journal of Biomolecular Screening*, *8*(2), 210–215. doi: 10.1177/1087057103252618
23. Li, Y., Li, P.-K., Roberts, M. J., Arend, R. C., Samant, R. S., & Buchsbaum, D. J. (2014). Multi-targeted therapy of cancer by niclosamide: A new application for an old drug. *Cancer Letters*, *349*(1), 8–14. doi: 10.1016/j.canlet.2014.04.003
24. Mackillop, W. J., Ciampi, A., Till, J. E., & Buick, R. N. (1983). A Stem Cell Model of Human Tumor Growth: Implications for Tumor Cell Clonogenic Assays2. *JNCI: Journal of the National Cancer Institute*. doi: 10.1093/jnci/70.1.9
25. Mendonsa, A. M., Na, T.-Y., & Gumbiner, B. M. (2018). E-cadherin in contact inhibition and cancer. *Oncogene*, *37*(35), 4769–4780. doi: 10.1038/s41388-018-0304-2
26. Mohandas KM, Desai DC: Epidemiology of digestive tract cancers in India. V. Large and small bowel. Indian J Gastroenterol 1999, 18:118-121.
27. Naksuriya, O., Steenbergen, M. J. V., Torano, J. S., Okonogi, S., & Hennink, W. E. (2016). A Kinetic Degradation Study of Curcumin in Its Free Form and Loaded in Polymeric Micelles. *The AAPS Journal*, *18*(3), 777–787. doi: 10.1208/s12248-015-9863-0
28. Neeley, C. (2016, July 7). Reducing the edge effect. Retrieved March 3, 2017, from https://www.thermofisher.com/blog/cellculture/reducing-the-edge-effect/

29. Niclosamide. (n.d.). Retrieved April 11, 2020, from https://www.caymanchem.com/search?q=niclosamide
30. Niclosamide (Oral Route) Description and Brand Names. (2020, February 1). Retrieved March 30, 2020, from https://www.mayoclinic.org/drugs-supplements/niclosamide-oral-route/description/drg-20065068
31. Odunsi, K., Matsuzaki, J., James, S. R., Mhawech-Fauceglia, P., Tsuji, T., Miller, A., … Karpf, A. R. (2014). Epigenetic Potentiation of NY-ESO-1 Vaccine Therapy in Human Ovarian Cancer. *Cancer Immunology Research*, *2*(1), 37–49. doi: 10.1158/2326-6066.cir-13-0126
32. Orange Book: Approved Drug Products with Therapeutic Equivalence Evaluations. (n.d.). Retrieved April 19, 2020, from https://www.accessdata.fda.gov/scripts/cder/ob/index.cfm
33. Ovarian Cancer Statistics – Ovarian Cancer Research Alliance. (n.d.). Retrieved December 30, 2017, from https://ocrfa.org/patients/about-ovarian-cancer/statistics/
34. Ovarian Cancer Treatment: How to Treat Ovarian Cancer. (n.d.). Retrieved November 30, 2017, from https://www.cancer.org/cancer/ovarian-cancer/treating.html
35. Radiation Therapy. (n.d.). Retrieved March 31, 2020, from https://www.cancer.org/treatment/treatments-and-side-effects/treatment-types/radiation.html
36. Ramus, S. J., & Gayther, S. A. (2009). The Contribution of BRCA1 and BRCA2 to Ovarian Cancer. *Molecular Oncology*, *3*(2), 138–150. doi: 10.1016/j.molonc.2009.02.001
37. Rayfield, W. J., Kandula, S., Khan, H., & Tugcu, N. (2017). Impact of Freeze/Thaw Process on Drug Substance Storage of Therapeutics. *Journal of Pharmaceutical Sciences*, *106*(8), 1944–1951. doi: 10.1016/j.xphs.2017.03.019
38. Terlikowska, K., Witkowska, A., Zujko, M., Dobrzycka, B., & Terlikowski, S. (2014). Potential Application of Curcumin and Its Analogues in the Treatment Strategy of Patients with Primary Epithelial Ovarian Cancer. *International Journal of Molecular Sciences*, *15*(12), 21703–21722. doi: 10.3390/ijms151221703
39. Thomson, J. A., Itskovitz-Eldor, J., Shapiro, S. S., Waknitz, M. A., Swiergiel, J. J., Marshall, V. S., & Jones, J. M. (1998). Embryonic Stem Cell Lines Derived from Human Blastocysts. *Science*, *282*(5391), 1145–1147. doi: 10.1126/science.282.5391.1145
40. Vallianou, N. G., Evangelopoulos, A., Schizas, N., & Kazazis, C. (2015). Potential Anticancer Properties and Mechanisms of Action of Curcumin. *International Journal of Cancer Research and Treatment*, *35*(2), 645–651.
41. Vector Builder. (n.d.). Retrieved from https://v1.vectorbuilder.com/vector/VB160216-10057/?format=pdf&annotation_uuid=

42. Waters JC, Chen RH, Murray AW, Salmon ED J *Cell Biol*. 1998 Jun 1; 141(5):1181-91
43. Weaver, B. A. (2014). How Taxol/paclitaxel kills cancer cells. *Molecular Biology of the Cell*, 25(18), 2677-2681. doi:10.1091/mbc.e14-04-0916
44. What is the meaning of * or ** or *** in reports of statistical significance from Prism or InStat? (n.d.). Retrieved April 6, 2020, from https://www.graphpad.com/support/faq/what-is-the-meaning-of--or--or--in-reports-of-statistical-significance-from-prism-or-instat/
45. Xu, T., Close, D., Price, S., & Sayler, G. (n.d.). High-Throughput Detection of Estrogenic Compounds Using ... Retrieved April 14, 2020, from https://490biotech.com/wp-content/uploads/2016/10/High-Throughput-Detection-490-BioTech.pdf
46. Yallapu, M. M., Maher, D. M., Sundram, V., Bell, M. C., Jaggi, M., & Chauhan, S. C. (2010). Curcumin induces chemo/radio-sensitization in ovarian cancer cells and curcumin nanoparticles inhibit ovarian cancer cell growth. *Journal of Ovarian Research, 3*(1), 11. doi:10.1186/1757-2215-3-11
47. Yo, Y.-T., Lin, Y.-W., Wang, Y.-C., Balch, C., Huang, R.-L., Chan, M. W. Y., … Lai, H.-C. (2012). Growth Inhibition of Ovarian Tumor-Initiating Cells by Niclosamide. *Molecular Cancer Therapeutics*, *11*(8), 1703–1712. doi: 10.1158/1535-7163.mct-12-0002
48. Yoo, S., Kim, K., Nam, H., & Lee, D. (2018). Discovering Health Benefits of Phytochemicals with Integrated Analysis of the Molecular Network, Chemical Properties and Ethnopharmacological Evidence. *Nutrients*, *10*(8), 1042. doi: 10.3390/nu10081042